Aus dem Max-Planck-Institut für neurologische Forschung
mit Klaus-Joachim-Zülch-Laboratorien der Max-Planck-Gesellschaft
und der Medizinischen Fakultät der Universität zu Köln
Direktor: Universitätsprofessor Dr. med. D. Y. von Cramon

Targeting developmental signalling pathways in experimental gliomas by overexpression of NUMB

Inaugural-Dissertation zur Erlangung der Doktorwürde
der Hohen Medizinischen Fakultät
der Universität zu Köln

vorgelegt von
Philipp Euskirchen
aus Bonn

promoviert am 1. Juni 2011

Gedruckt mit Genehmigung der Medizinischen Fakultät der Universität zu Köln, 2011.
Druck: Druckhaus Berlin Mitte, Berlin.

Dekan: Universitätsprofessor Dr. med. Dr. h. c. Th. Krieg

1. Berichterstatter: Professor Dr. med. A. Jacobs

2. Berichterstatter: Universitätsprofessor Dr. med. R. Goldbrunner

Erklärung

Ich erkläre hiermit, dass ich die vorliegende Dissertationsschrift ohne unzulässige Hilfe Dritter und ohne Benutzung anderer als der angegebenen Hilfsmittel angefertigt habe; die aus fremden Quellen direkt oder indirekt übernommenen Gedanken sind als solche kenntlich gemacht.

Bei der Auswahl und Auswertung des Materials sowie bei der Herstellung des Manuskriptes habe ich keine Unterstützungsleistungen erhalten.

Weitere Personen waren an der geistigen Herstellung der vorliegenden Arbeit nicht beteiligt. Insbesondere habe ich nicht die Hilfe einer Promotionsberaterin oder eines Promotionsberaters in Anspruch genommen. Dritte haben von mir weder unmittelbar noch mittelbar geldwerte Leistungen für Arbeiten erhalten, die im Zusammenhang mit dem Inhalt der vorgelegten Dissertationsschrift stehen.

Die Dissertationsschrift wurde von mir bisher weder im Inland noch im Ausland in gleicher oder ähnlicher Form einer anderen Prüfungsbehörde vorgelegt.

Köln, 27. September 2010

Die in dieser Arbeit angegebenen Experimente sind nach entsprechender Anleitung durch Herrn Dr. Dr. Hrvoje Miletic von mir selbst ausgeführt worden.

Acknowlegdements

Many people have directly or indirectly contributed to this thesis. I would like to thank them.

First of all, I would like to thank Dr Hrvoje Miletic for the proposal of this project and its dedicated supervision including dozens of hours of discussions.

I would especially like to thank Professor Dr Rolf Bjerkvig for the opportunity to work in his laboratory, scientific guidance and mentoring.

I am very grateful to Professor Dr Andreas Jacobs for the supervision and support that made this thesis possible.

Importantly, I want to thank all my colleagues in Bergen and Cologne, especially Narve Brekkå, Kai-Ove Skaftnesmo, Tor-Christian Johannessen and Anke Söntgerath for sharing their practical and theoretical knowledge, their collaboration and fruitful discussions.

Furthermore, I am indebted to all collaborators who have contributed their expertise, offered me teaching and provided materials. I am especially grateful to Privatdozentin Dr Katrin Lamszus and Dr Hauke Günther (University Hospital Hamburg-Eppendorf) for providing gliomaspheres and relevant teaching, Professor Dr Dorothee van Laer and colleagues (Georg-Speyer-Haus, Frankfurt) for providing viral backbones and sharing their expertise on virus production, and Professor Dr Josef Beuth (University of Cologne) for use of the flow cytometry facility.

I would also like to thank Volker Neuschmelting for proof-reading the manuscript. Thanks to Monica Hellesøy for all the coffee breaks, and — a very special thank you to Hanne Welper for invaluable moral support.

Finally, I would like to thank my family for encouraging and supporting me at all times.

Table of contents

1. Introduction **10**

1.1. Glioblastoma multiforme 11
1.2. Cancer stem cells 12
1.3. Asymmetric cell division 16
1.4. Mechanisms of NUMB action 16
1.5. NUMB as a tumor suppressor 19
1.6. Glioma models 20
1.7. Aims of the study 22

2. Material and methods **23**

2.1. Patient material 23
2.2. Cell culture 23
2.3. Cloning of plasmids 24
2.3.1. Cloning of Numb lentiviral vectors 24
2.3.2. Subcloning of Shh and Gli1 plasmids 24
2.4. Growth assays 25
2.5. Western blotting 25
2.6. Realtime PCR 26
2.7. Luciferase reporter assays 27
2.8. Immunocytochemistry 27
2.9. Flow cytometry 28
2.10. Virus production 29
2.10.1. Production 29
2.10.2. Ultracentrifugation 29
2.10.3. Titration 30
2.11. Animal experiments 30
2.11.1. Intracranial tumor implantation 30
2.11.2. Magnetic resonance imaging 31
2.11.3. Survival analysis 31
2.11.4. Immunohistochemistry 31
2.12. Microarray data and analysis 32
2.13. Statistics 32

3. Results **33**

3.1. NUMB expression in patient material 33
3.2. Differential expression of NUMB isoforms in adherent glioma cell lines 33

3.3. Generation of NUMB lentiviral vectors 35
3.4. Generation of U87-NUMB cell lines 37
3.5. Unchanged proliferation in cell culture 38
3.6. No induction of differentiation by NUMB in U87 40
3.7. NUMB transduced U87 cells are tumorigenic in vivo 41
3.8. Regulation of signalling pathways by NUMB in adherent glioma cell lines . . . 43
3.9. NUMB expression in gliomaspheres 45
3.10. NUMB does not change morphology of cancer stem-like glioma cells 47

4. Discussion **49**
4.1. NUMB expression in patient samples and cell lines 49
4.2. Overexpression of NUMB in adherent glioma cell lines 50
4.3. Pathway interactions in experimental gliomas 51
4.4. Model considerations 53
4.5. NUMB overexpression in gliomaspheres 54
4.6. Conclusions 55

5. Summary **56**

6. Zusammenfassung **58**

7. References **61**

A. Appendix **71**
A.1. Manufacturers and suppliers 71
A.2. Plasmid map 73
A.3. Virus batches 74

Glossary

BCA	bicinchoninic acid
BDNF	brain derived neurotrophic factor
bFGF	basic fibroblast growth factor
BSA	bovine serum albumine
cDNA	complementary DNA
CMV	cytomegaly virus
CSC	cancer stem cell
CT	computer tomography
DAPI	4',6-diamidino-2-phenylindole
DMEM	Dulbecco's Modified Eagle Medium
DMSO	dimethyl sulfoxide
DNA	deoxyribunleic acid
EGF	epidermal growth factor
eGFP	enhanced green fluorescent protein
EGFR	epidermal growth factor receptor
FBS	fetal bovine serum
FCS	fetal calf serum
GAPDH	glyceraldehyde 3-phosphate dehydrogenase
GBM	glioblastoma multiforme
GFAP	glial fibrillary acidic protein
GFP	green fluorescent protein
HIV	human immunodeficiency virus
ICP	intracranial pressure
IHC	immunohistochemistry
MGMT	O-6-methylguanine-DNA methyltransferase
MOI	multiplicity of infection
MRI	magnetic resonance imaging
mRNA	messenger RNA
NGF	nerve growth factor
NHB	normal human brain
NSC	neural stem cell
PBS	phosphate buffered saline
PCR	polymerase chain reaction
PFA	paraformaldehyde

PMT	photomultiplier
PRR	proline rich region
PTB	phospho tyrosine binding
RA	retinoic acid
RNA	ribonucleic acid
SHH	sonic hedgehog
SOP	sensory organ progenitor
TBS	Tris buffered saline
TMZ	temozolomide
VEGF	vascular endothelial growth factor
VSV-G	vesicular stomatitis virus G protein
WB	western blotting
WHO	World Health Organization

1. Introduction

Glioblastoma multiforme (GBM) is the most frequent and most aggressive primary brain tumor in adults. It is characterized by rapid, highly infiltrative growth and early recurrence after treatment. Despite intensive research and multimodal treatment including surgical resection, radiotherapy and chemotherapy, patients today still face a dismal prognosis with a median survival of 14.6 months [83].

Recent work on the genetics and biology of cancer in general and on the tumorigenesis of brain tumors in particular has shed new light on the development of this fatal disease, partly explaining failure of current therapies. The identification of *cancer-initiating cells*, or *cancer stem cells (CSCs)*, in malignant gliomas [79] as well as in other tumors, a subpopulation of cells within the tumor that is capable of self-renewal and multilineage differentiation, provides the basis for a novel understanding of cancer.

According to this stem cell theory of cancer, only this minor portion of tumor cells acts as the motor of the disease. Cancer stem cells have also been shown to be more resistant to DNA damage induced by radiotherapy [7] and chemotherapy [58] than non stem-like cells. Failing to eliminate those cells will lead to failure of therapy. Even worse, ineffective therapies might drive the selection of cancer-stem cells and therefore explain early recurrence of tumors. Additionally, none of the current therapies take into account the heterogeneity of cancer cells.

Stem cells use asymmetric cell division for self-renewal and it is likely that the same mechanism is used by CSCs. Also, the same signalling machinery to communicate self-renewal and differentiation is shared by normal and malignant cells. The cell fate determinant NUMB is a gene that plays a key role during self-renewal of stem cells. Asymmetric segregation of NUMB during cell division determines cell fate and has been conserved from Drosophila to mammals (reviewed in [18]). Mechanistically, its effects are mediated by a number of signalling pathways which are also known to be active in gliomas.

The goal of this thesis was to deplete CSCs in experimental gliomas by interfering with asymmetric cell division and the signalling pathways behind by forced expression of NUMB in tumor cells in vitro and in vivo.

1.1. Glioblastoma multiforme

Epidemiology and classification of brain tumors The incidence of brain tumors is approximately 15 per 100,000/year and glioblastoma multiforme (GBM) accounts for about 25% of all cases. Men are more likely to be affected than women. Primary tumors of the central nervous systems are grouped by their putative cell of origin and graded by histological criteria into four prognostically relevant groups (WHO I - IV) [50].

GBM belongs to the group of astrocytic tumors and is classified as WHO IV. The frequently used term malignant glioma refers to glial (astrocytic and oligodendroglial) grade III and IV tumors. Further classification based upon certain molecular markers or transcription profiling (e.g. [64]) have been proposed but are not used in the clinic yet. Merely MGMT promoter methylation, a strong predictor of response to certain chemotherapeutic drugs, and 1p/19q co-deletions in oligodendroglioma are analyzed in some clinics. GBM can arise de novo as primary GBM (about 80% of cases) or from less malignant tumors, e.g. anaplastic astrocytoma (secondary GBM) [44].

Diagnosis Clinical symptoms vary based upon the localization of the tumor mass. Early symptoms may be unspecific, such as headache or personality changes. More specific symptoms include epileptic seizures, disturbed vision, aphasia and paresis. However, due to the rapid growth of GBM, the first symptoms are often caused by elevated intracranial pressure (ICP), such as matutinal vomiting, disturbed vigilance, headache or pathological grasp reflexes as very early signs of increased ICP.

The tumor is usually diagnosed by imaging modalities, namely computer tomography (CT) and magnetic resonance imaging (MRI). On MRI scans, T2 weighted images show an inhomogenous tumor, often with surrounding edema. Contrast enhanced images often display a hyperintense tumor margin, indicating disruption of the blood brain barrier. A final diagnosis can only be achieved by open or stereotactic biopsy and histology.

Histologically, GBM is characterized by nuclear aplasia, mitotic figures, necrosis, pseudopalisading and angiogenesis [50]. Routine immunohistochemistry includes Ki67 (also known as MIB-1) labelling and glial fibrillary acidic protein (GFAP) expression, which can vary considerably from tumor to tumor and even within the tumor.

Therapy and prognosis Current treatment combines surgical resection with adjuvant chemotherapy and concomitant radiotherapy. Most GBMs can not be resected entirely due to infiltration of important functional regions of the brain. Thus, adjuvant therapy is inevitable to delay relapse.

Introduction of temozolomide as standard chemotherapy in glioma treatment has slightly improved survival and some mid-term survivors have benefitted remarkably [83, 82]. Response to temozolomide (TMZ) is dependent on the activity of the enzyme O-6-methylguanine-DNA methyltransferase (MGMT) and promotor hypermethylation often inactivates MGMT in GBM [33].

Experimentally, therapies are directed against angiogenesis or known molecular targets (e.g. EGFR). Examples are monoclonal antibodies against epidermal growth factor receptor (EGFR), which is frequently amplified or mutated in GBM, or vascular endothelial growth factor (VEGF) in order to target angiogenesis. Suicide gene therapy has been evaluated in several clinical trials (cite: gene therapy trials register) without convincing results.

1.2. Cancer stem cells

The cancer stem cell hypothesis claims that there exists a subpopulation of cells within a tumor which is solely capable of recapitulating the tumor. It postulates that cells in this subpopulation fulfill the operational definition of a stem cell. A stem cell is capable of

(i) self-renewal and

(ii) multi-lineage differentiation.

These CSCs generate a heterogenous tumor with most daughter cells not fulfilling stem cell criteria. The theory contrasts the traditional paradigm that cancer evolves by clonal expansion of a single mutated cell generating identical offspring. It is based upon observations that cells selected for certain molecular markers are tumorigenic when xenografted into animals while the remaining cells are not. This phenomenon was first observed in malignant diseases of the hematopoetic system [15]. Since then, it has been investigated in a variety of solid tumors, including malignant gliomas [79].

Many issues are discussed or implicated in the context of the cancer stem cell hypothesis. The following enumeration mentions some of the issues touched by CSC research in gliomas and other cancers (references are examples).

- The CSC theory suggest that a glioma's cell of origin is a stem cell [34].
- CSCs only make up a minor fraction of the entire tumor bulk [16].
- CSCs divide slowly [48].
- Developmental signalling pathways are active in CSCs [8, 31].

- CSCs are more resistant to stress such as hypoxia, radiation or chemotherapy [7, 58].
- CSCs can be identified by certain molecular markers (usually surface proteins) [79].
- A tumor is an organ-like structure with hierarchical organization [15].

Because of this large number of statements it is reasonable to distinguish between three main aspects:

(i) the cell of origin debate

(ii) heterogeneity and hierarchy of cancer cells

(iii) the signalling pathways and molecular mechanisms that are shared by cancer cells and stem cells

Cell of origin Taking into account the observations mentioned so far, it is indeed an intuitive conclusion that cancer might evolve from mutated progenitor or stem cells. It has been shown that germline mutations of tumor suppressor genes (such as PTEN or p53) will first affect progenitor cells [49].
On the other hand, Bachoo and colleagues demonstrated that combined INK/ARF deletion renders astrocytes tumorigenic [4]. Thus, it is also possible that genomic instability in any mutated cell drives de-differentiation and cells can regain stem cell properties. This is not unlikely, especially since research aiming to utilize stem cells for therapy has proven that experimental reprogramming of differentiated cells even into embryonic stem cells is feasible and can be achieved by reexpression of a handful of transcription factors [84].

Heterogeneity Until a decade ago, it was assumed that all cancer cells within a tumor are equally tumorigenic. The CSC theory now suggests that tumors rather resemble organs with a small fraction of slowly dividing stem-like cells giving birth to a large number of daughter cells which have high but limited proliferative activity and a more differentiated phenotype. In this scenario, only the minority of stem-like cells is capable of forming a new tumor.

Much attention has been paid to the small CSC population, its clonogenic properties in vitro and in vivo, chemoresistance and molecular fingerprint. The microenvironment of CSCs, termed stem cell niche, and interaction with endothelial cells have been studied [16]. However, little is known (at least for CNS tumors) about the majority of non-CSC cells with respect to this new model of cancer. No studies have been published that aim to unravel the relationships between CSCs and the remaining tumor and to trace the fate of CSC daughter cells.

Signalling pathways Regardless of the two issues adressed so far, there is convincing evidence that cancer cells make use of metabolic and signalling pathways that are commonly used by stem cells. For example, anaerobic glycolysis is frequently observed in stem cells. From an evolutionary point of view, this is reasonable for these cells in order to reach locations of tissue damage where oxygen supply is impaired. In cancer cells with a stem-like phenotype, utilisation of this metabolic pathway has also been observed [85].

So-called developmental signalling pathways, such as Notch, Hedgehog, BMP or Wnt signalling have been shown to be active in numerous cancers. A growing body of evidence suggests this to be the case in gliomas as well. Drugs interfering with these pathways are in preclinical testing. For example, in medulloblastomas, Notch signalling can be repressed using a γ-secretase inhibitor [27]. In GBM, cyclopamine can inhibit growth of experimental gliomas by Hedgehog pathway blockade [8].

However, the term 'developmental' signalling pathways might be misleading and should maybe considered historical based upon the context of their discovery because most of these pathways appear to be universal and play important roles during adult life as well.

Nevertheless, utilization of these functional components of a cell's molecular machinery is frequently found in stem cells. One assumption that is central to this thesis as well, is that all of these properties might be orchestrated and governed by certain molecular mechanisms determining a stem cell phenotype (such as transcription factors or epigenetic regulation).

Stem cell markers An important question in cancer stem cell research is how the small population of interest can be distinguished from the majority of non-stem cells. A variety of stem cell markers identified by developmental neurobiologists has been shown to be expressed in brain tumor stem cells to illustrate their stem cell phenotype.

CD133 At first, CD133 was introduced as a marker for separation of cancer initiating cells from the remaining tumor cells. Because of its localization on the cell surface, it can easily be used for live cell sorting. Some pitfalls exist, for example because CD133 is easily cleaved by proteases such as trypsin which are frequently used for dissociation of tumor samples before sorting, increasing the number false-negative results. Later, several studies have shown that CD133-negative cells give rise to tumors as well [10, 88]. Recently, CD133 has been associated with response to hypoxia [30].

Hoechst 33342 exclusion Another method used for enrichment of putative cancer stem cells is the exclusion of Hoechst 33342 dye. It can diffuse through cell membranes, thus primarily labelling all cells. Due to expression of ABC transporters, which are capable of pumping a variety of substrates out of the cytoplasm, some cells can actively efflux

the dye (commonly referred to as *side population*). Expression of ABCG2 has been associated with a stem-like phenotype [95] and also been suggested to be responsible for drug resistance in various tumors [35].

Nestin Nestin has been observed to be exclusively expressed in a number of neural progenitor cells. However, nestin is expressed abundantly in glioma cell lines and also in spheroid glioma models [69]. On the other hand, one study reports very low percentages of nestin-positive cells in GBM and other primary brain tumors [16], so there is some controversy whether nestin is a GBM or a CSC marker.

SOX2 The transcription factor SOX2 is frequently reported to be expressed in glioma stem cells. However, due to its nature as a nuclear protein, it is not accessible for live cell staining.

Musashi-1 Musashi-1 has been linked to asymmetric cell divisions in Drosophila and is also expressed in mammalian neural progenitor cells. Importantly, it directly interacts with NUMB (see Section 1.4).

OLIG2 Not exactly a stem cell marker, OLIG2 is physiologically expressed in lineage committed oligodendrocytic progenitor cells. Its expression in gliomas is not restricted to cells with a stem-like phenotype, but it seems to be required in CSCs [48].

CD15 Recently, CD15 has been proposed as a marker of cancer stem cells in medulloblastoma, being superior to CD133 [67]. No data exist for astrocytic tumors so far.

BrdU labelling This method has not been used in the context of glioma research, but it should be mentioned because of its popularity in developmental neuroscience. In search for slowly dividing cells, many studies have employed incorporation of the nucleotide analogon BrdU to mark cells in S phase. Putative progenitor cells were then identified in the BrdU-negative population (e.g. [77]). The advantage of this method is that it can be used in vivo by addition of BrdU to the drinking water of animals. However, because staining of BrdU requires permeabilization, it does not allow for selection of live cells.

None of the markers above have proven to be reliable markers of cancer-initiating cells in gliomas. However, their expression in tumor material underscores the similarity of some cancer cells to neural progenitors and thus gives support for the assumption that stem-cell related particularities could be exploited for therapy.

1.3. Asymmetric cell division

Development and maintenance of tissues and organs is a complex process tightly regulated by the participating cells in a spatiotemporal manner. Despite of this complexity, the underlying principles are not complicated. Communication between cells is provided by developmental signalling pathways whose function depends on the context they act within, and only a handful of these evolutionary highly conserved mechanisms gives rise to the enormous complexity of multicellular organisms.

Stem cells play a key function in this scenario. They give rise to a variety of cell types that eventually make up the tissue. At the same time, a constant pool of stem and progenitor cells is maintained through adulthood for regular turnover (especially in the epithelium of skin and mucosa) and tissue repair. The number of stem cells and birth of progeny is regulated by symmetric and asymmetric cell division. Symmetric cell division can give birth to either two stem cells thus expanding their number or two daugther cells who will eventually differentiate. In turn, asymmetric cell division will give rise to one stem cell and a differentiating cell and this keeps the stem cell pool at constant size.

One of the key regulators of this mechanism is NUMB. The protein is asymmetrically segregated at mitosis, so the daughter cells inherit different amounts of NUMB. Importantly, it has been shown that *numb* orchestrates differentiation of Drosophila sensory organ progenitor cells. *numb* mutant flies failed to form properly differentiated sensory organs, while *numb* overexpressing cells underwent differentiation too early [18].

The picture gets more complicated in mammals. During early stages of murine neurogenesis, Numb is involved in maintaining the stem-like properties of neural progenitor cells [63] and also controls stem cell numbers in the developing nervous system [38]. Later on during CNS ontogenesis, it was observed that Numb is expressed in differentiated cells such as neurons [87]. These contrary effects are likely due to the existence of different mammalian Numb isoforms which seem to promote either differentiation or proliferation [25, 6, 87].

The idea that overexpression of NUMB could eventually lead to differentiation is the fundamental concept of this thesis.

1.4. Mechanisms of NUMB action

Structurally, NUMB contains several binding sites (PTB and PDZ domains) for interaction with other proteins but does not display any enzymatic activity itself. NUMB rather serves as a scaffold for interacting proteins. Some biochemical reactions require close proximity of the participating molecules which is mediated by NUMB. This also allows restriction

of enzymatic reactions to certain subcellular sites, for example by membrane association of NUMB. Given its own asymmetric distribution during cell division, it can promote different cell fates to the two daughter cells generated. NUMB has been described to promote mainly two types of reactions:

Ubiquitylation Ubiquitin is a 9 kD protein present (as the name suggests) in all eukaryotic cells. It can be bound covalently to other proteins which marks the protein for degradation by proteasomes. NUMB can mediate the transfer of ubiquitin to target proteins which is done by a class of enzymes termed *E3 ligases*. Doing so, ubiquitin and NUMB regulate protein half-life and can influence the kinetics of intracellular signalling.

Endocytosis A second mechanism is interaction with endocytic processes. NUMB binds to several endocytosis related proteins such as Eps15 [70] and AP2 [71]. This mechanism seems to be important for cell fate decisions, but also in developing neurons for axon growth [60].

In the literature, NUMB is mentioned in the context of several signalling pathways. For the most part, these pathway interactions have been first discovered in Drosophila and were then found to be conserved in mammals and humans. If not stated explicitly, human pathways and genes are referred to in this thesis. Referral to human genes is further emphasized by upper-case gene symbols.

Notch signalling The Notch pathway is crucial for differentiation processes during development [3]. It mediates signals to neighbouring cells by membrane-bound ligands and receptors. The ligands include *delta-like* and *jagged* genes, i.e. DLL1 through DLL6 as well as JAG1 and JAG2. They associate with the NOTCH1 through NOTCH4 receptors on the target cell, a class of trans-membrane proteins. Upon activation, the intracellular domain of NOTCH1 is cleaved by the γ-secretase complex and can translocate to the nucleus where it activates transcription factors that promote the transcription of Notch target genes. This CSL complex activates HES1 through HES5 which subsequently upregulate target genes involved in a wide variety of processes in different organs. During neurogenesis, active NOTCH signalling usually maintains stem-cell properties in progenitor cells.

A solid body of evidence suggests that NUMB antagonizes NOTCH signalling. This is achieved by promoting endocytic trafficking of NOTCH1 from the cell membrane into cytoplasmic vesicles [55]. Subsequently, NUMB can induce ubiquitin-mediated degradation of NOTCH1 through the E3 ligase ITCH [56].

NOTCH signalling also seems to be important in gliomas. Experimentally, it could be demonstrated that components of the NOTCH pathway are expressed in glioma cell lines

and biopsy material [66, 40]. Knockdown of NOTCH1 inhibits proliferation in vitro and prolongs survival when cells were xenografted into mice [66]. A recent study reports that EGFR, which is frequently amplified or overexpressed in gliomas, interacts with Notch signalling in neural stem cells (NSCs) in a NUMB-dependent manner [2]. It has also been shown that Notch signalling upregulates expression of the stem cell marker nestin [76].

Querying the REMBRANDT database [51], a collection of glioma gene expression and clinical data, shows that high levels of HES1 correlate with shortened survival of glioma patients (Figure 1.1).

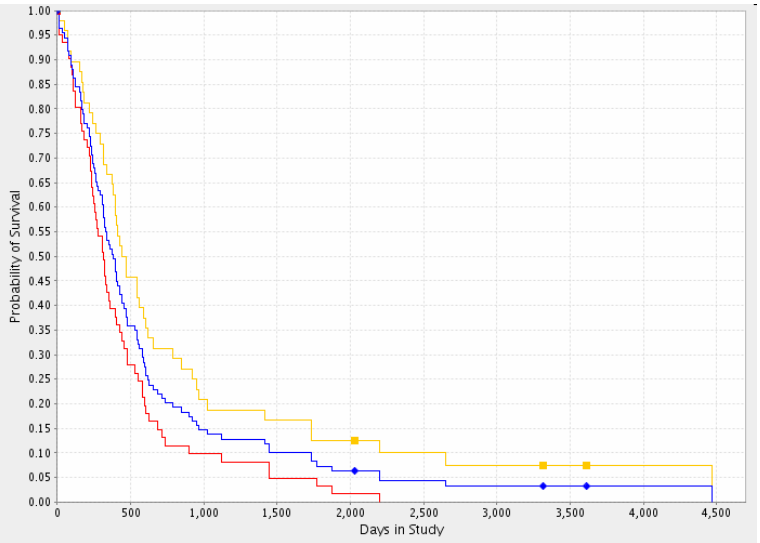

Figure 1.1.: **HES1 mRNA levels correlate with patient survival.** Survival of GBM patients with high (*red*), intermediate (*blue*) or low (*yellow*) levels of HES1. (National Cancer Institute, 2005. REMBRANDT <http://rembrandt.nci.nih.gov>. Accessed 2009 July 3.)

It should be noted, however, that not all NOTCH pathways components necessarily have the same effects. One study predicted longer survival by DLL3 levels [64], and NOTCH1 and NOTCH2 receptors were reported to have antagonistic effects in embryonal brain tumors [28].

Hedgehog signalling The Hedgehog pathway is another highly conserved signalling cascade, regulating the maintenance of stem cells and organizing their differentiation. It can achieve long-distance communication by its solube ligands sonic hedgehog (SHH), desert hedgehog (DHH) and Indian hedgehog (IHH), which bind to *patched* receptors (PTCH1 and PTCH2 in humans). Upon ligand binding, PTCH and SMO dissociate and SMO can translocate to the nucleus, where it initiates production of transcription factors GLI1 through GLI3.

The pathway has been shown to be modulated by NUMB [53]. Similar to Notch signalling, NUMB promotes ubiquitylation of GLI1 by ITCH, and GLI1 is then degraded by proteasomes. In this study, it was also shown that NUMB is downregulated in medulloblastomas, another primary brain tumor, and that overexpression of NUMB in medulloblastoma cell lines can inhibit their growth. Similar results have been published for gliomas. A recent study showed that active Hedgehog signalling is correlated with shorter survival of GBM patients [90]. In experimental gliomas, self-renewal of CD133+ cells could be inhibited by knock-down of SMO or chemically blocking the pathway using cyclopamine [20]. Both strategies resulted in reduced tumorigenicity of xenografts in nude mice.

Tumor suppressor p53 The tumor suppressor p53, also named the "guardian of the genome", has important functions regarding DNA damage including induction of repair mechanisms, cell cycle arrest and induction of apoptosis.

One study suggests that NUMB interacts with p53 by entering a tri-complex consisting of NUMB, p53 and its negative regulator MDM2 [21]. p53 is supposed to be stabilized by this interaction, resulting in a tumor suppressor function for NUMB.

NUMB is also supposed to interact directly with MDM2. It was found that NUMB is a ubiquitylation target of E3 ligase MDM2 itself [92]. Additionally, another study found that MDM2 mediates translocation of NUMB to the nucleus [39].

Musashi-1 Musashi-1 (MSI1) is a stem cell marker frequently expressed in neuronal stem and progenitor cells [29]. Translation of NUMB is inhibited by MSI1 by interacting with the 3'-untranslated region of NUMB mRNA [37].

Taken together, NUMB is involved in a number of glioma relevant pathways (Figure 1.2). This does not mean that NUMB function itself is disturbed in cancer (for example, by mutation of its nucleotide sequence). It rather happens to be in a central position controlling mechanisms and pathways frequently used by (cancerous) stem cells, thus making it a possible therapeutic target.

1.5. NUMB as a tumor suppressor

Few studies have examined whether NUMB might play a role in the process of tumorigenesis. Pece and colleagues found that loss of NUMB expression in histological sections of tumor samples was correlated with poor survival of breast cancer patients [62]. In the same

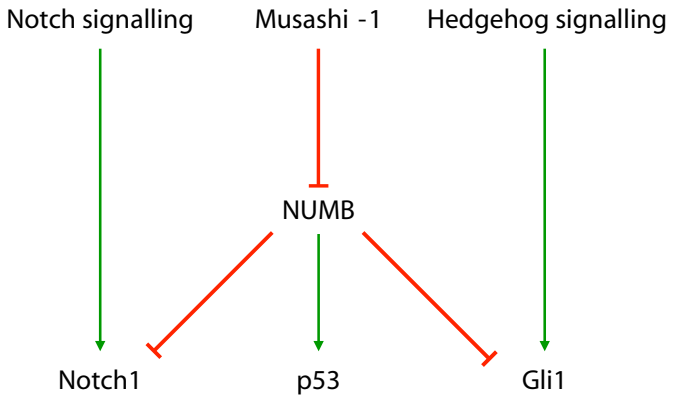

Figure 1.2.: **Overview of NUMB interactions** Arrows indicate activation (*green*) or inhibition (*red*) of downstream targets.

study, overexpression of NUMB in mammary cancer cell lines with low endogenous levels of NUMB inhibited proliferation and rendered cells more sensitive to chemotherapeutic treatment.

Similarily, loss of NUMB expression was found in about 30% of samples of non small cell lung cancer [89]. In these tumors, NUMB expression correlated inversely with Notch pathway activity. In hematopoietic malignancies, it has been shown that the proportion of cancer stem cells was reduced by overexpression of NUMB. This effect was linked to activity of Hedgehog signalling [93]. Additionally, NUMB expression is inversely correlated with Ki-67 immunoreactivity and histological grade in salivary gland carcinomas [52].

Literature regarding the function of NUMB in glioma is sparse and controversial. One study suggests a role for Numb in human glioma [19] through ligand of Numb protein X (LNX) which has been found to be downregulated in gliomas in this work. Supposedly, LNX mediates the translocation of Numb from the nucleus to the cytoplasm, its site of action. However, another study describes ubiquitination of Numb by LNX which promotes protein degradation, thus proposing a contrary effect of LNX on Numb [59]. Finally, NUMB expression in histological samples of gliomas was briefly characterized, showing that NUMB is expressed in paraffin sections of astrocytic tumors from grade I to IV [91].

1.6. Glioma models

The study of malignant gliomas depends on experimental models that are suited to answer the questions being asked. Many models of glioma exist and they serve different purposes and meet different needs. In this study, different glioma models were used and compared. Therefore, a brief introduction shall be given. In general, two entirely different kinds of

glioma models can be distinguished, those aiming to recapitulate a typical phenotype of GBM (such as its histopathology) and those focusing on its pathogenesis. The purpose of the first ones is to establish an experimental tumor closely resembling patient tumors which can be used for an intervention, such as chemotherapeutic treatment. The latter models manipulate healthy cells in order to see if this intervention turns them into tumors.

Phenotype-focused models Traditionally, primary cells from surgical samples are dissociated and grown in growth medium supplemented with serum. The resulting cell line usually proliferates quite fast, is easy to be handled, passaged and cryopreserved. A large subset of the human cell lines readily generates tumors in immunocompromised animals when implanted into the brain or even subcutaneously. These tumors recapitulate features of GBM such as angiogenesis and necrosis, but not invasion. However, most of the cell lines that are commonly used today were generated more than thirty years ago and it is very likely that the genomic background of the cells has changed over time.

Lately, researchers have started to establish cell lines in medium which was developed for expansion of neural stem cells [34, 78]. Although several different media are used, their common feature is the lack of serum and use of chemically well defined growth factors, usually epidermal growth factor (EGF) and basic fibroblast growth factor (bFGF). A subpopulation of cells generated under these conditions has been shown to fulfill the criteria of stem cells and provided the basis for the cancer stem cell hypothesis. Phenotypically, these cells form nonadherent sphere-like structures termed *neurospheres* or *gliomaspheres*.

It has been shown that these cells more closely resemble the genomic background of the parental tumor as do serum-cultured cells [47]. Further, serum-cultured cells give rise to clearly demarked tumors in vivo, while tumors from CSC-rich cell lines have turned out to be highly invasive [79, 47, 31].

Another model uses in vivo passaging and in vitro growth of spheroids in agar-coated flasks [14]. The model generates two distinct phenotypes in vivo: a highly invasive phenotype with stem-like properties and a less invasive, angiogenic phenotype [69]. It ranges between the two model systems mentioned before because it uses regular serum-containing medium but still generates stem-like phenotypes.

In summary, serum-cultured cell lines provide an easy and fast tool for in vitro and in vivo studies at the cost of important histological hallmarks (i.e. invasiveness) and genomic stability. On the other hand, serum-free cell lines are suited for the study of cancer stem cells, but neurospheres are more difficult to handle compared with monolayer cells. However, a recent study suggests that CSC-like glioma cell lines can be maintained as adherent monolayers without loss of multipotency or self-renewal capacity [65].

Pathogenesis-focused models The tumor models mentioned so far all aim to reflect morphological or functional features of gliomas and are thus preferred for translational research such as studies of chemotherapeutic agents, imaging modalities or new therapeutic approaches. However, pathogenesis of malignant glioma is still quite unclear. The debate about the cell of origin of these tumors is ongoing and despite advances in the field of genomic mutations the cause of genetic instability or which mutation might occur first is unknown.

Therefore several other models have been established to study these processes. It has been observed that in animals tumors can be induced by certain chemicals that induce DNA damage. For example, the C6 rat glioma cell line was generated by application of N-nitrosomethylurea [11]. Mouse or rat gliomas have the advantage to be isogenic and can be allografted into immunocompetent animals.

Lately, putative tumor suppressor genes or oncogenes were selectively targeted in order to generate brain tumors in mice or rats. For example, combined knockout of the INK4a and ARF loci resulted in malignant transformation of astrocytes [4]. Simultaneous deletion of tumor suppressors p53 and PTEN also generates glial tumors [94], and so do activation of Akt and Ras [36] or overexpression of PDGF [23].

1.7. Aims of the study

The aim of this thesis was to investigate whether NUMB could be exploited as a therapeutic agent for glioma gene therapy. Specifically, the following questions were asked:

- Does NUMB overexpression induce growth arrest or inhibit proliferation of glioma cells in vitro and in vivo?
- Does NUMB induce differentiation in experimental gliomas that can be assessed by expression of neuronal or glial markers, morphology or senescence?
- Is NUMB differentially expressed in gliomas compared to normal brain?
- Does NUMB expression correlate (inversely) with a stem-like phenotype?

2. Material and methods

2.1. Patient material

Protein lysates and cDNA from patient biopsies were kindly provided by Per Øyvind Enger (Department of Neurosurgery, Haukeland University Hospital, Norway). All samples were histologically confirmed GBM.

2.2. Cell culture

Adherent cell lines Human U87, U251 and U373 glioma cell lines were obtained from ATCC and grown in Dulbecco's Modified Eagle Medium (DMEM) (Sigma) supplemented with 10% fetal calf serum (FCS) (PAA), 100 U ml^{-1} penicillin/streptomycin (Lonza), 2 mM L-glutamine (Lonza) and 5 μg ml^{-1} plasmocin (Invivogen). Cells were grown in cell culture-coated flasks (Nunclon, Thermo Scientific) in a humidified 37 °C incubator with 5% CO_2 and passaged using Trypsin EDTA (Sigma).

Gliomaspheres GS-1, GS-2, GS-4, GS-5 and GS-9 cells were kindly provided by Katrin Lamszus, Hamburg [31]. Cells were grown in Neurobasal medium (Invitrogen) supplemented with B27 (Invitrogen), 20 ng ml^{-1} EGF (Peprotech), 20 ng ml^{-1} bFGF (Peprotech) and 32 IE ml^{-1} heparin (Ratiopharm). For passaging, spheroids were mechanically dissociated using a 200 μl pipette tip. Adherent cells were detached using Accutase (PAA).

Cryopreservation Cell lines grown under serum conditions were cryopreserved in complete medium containing 20% FCS and 10% DMSO (Sigma). Cryomedium used for neurospheres was fetal bovine serum with 10% DMSO. Neurospheres were frozen as single cell suspensions. Briefly, cells were centrifuged and growth medium was replaced by 1 ml cryomedium for each vial to be frozen. The cell suspension was transferred to cryotubes (Nunclon, Thermo Scientific) and kept at −80 °C for 24h, then moved to nitrogen tanks for long term storage.

For thawing, cells were quickly brought to room temperature. Cells were washed once in growth medium before transfer to cell culture flasks. Gliomaspheres frozen in FCS were washed twice to remove all traces of serum.

2.3. Cloning of plasmids

2.3.1. Cloning of Numb lentiviral vectors

The M107 eGFP lentiviral backbone was kindly provided by Dorothee von Laer (Georg-Speyer-Haus, Frankfurt, Germany) [13]. Human NUMB cDNA was cloned in-frame into a BamHI cloning site between the pCMV promotor and eGFP.

NUMB4 was amplified from total human fetal brain cDNA (BioChain). NUMB3 cDNA was provided by Joe Verdi (Center for Molecular Medicine, Maine Medical Center, USA). NUMB2 was synthesized by overlapping PCR using NUMB4 as template. NUMB1 cDNA was kindly provided by Salvatore Pece (European Institute of Oncology, Milan, Italy) [62].

NUMB cDNA was amplified by PCR (annealing temperature 60 °C, 40 cycles) using numbCloning-kozak primers and Phusion polymerase (Finnzymes). The primers were designed to append a Kozak consensus sequence (GCCACC) to the 5' end of the amplicon and a BglII restriction site to both ends.

Amplicons were digested with BglII and purified on a MinElute column (Qiagen). The M107 backbone was cut with BamHI, dephosphorylated using shrimp alkaline phosphatase (Promega, Madison, WI, USA (Promega)) and purified using Wizard SV columns (Promega). For ligation, vector and insert were fused at a ratio 3:1 or 4:1 using T4 ligase (Promega). Chemocompetent E. coli were then transformed by the heat-shock method. Bacteria were plated on LB agar plates with ampicillin (Sigma Aldrich, St. Louis, MO, USA (Sigma)) and incubated overnight at 37 °C. Colonies were picked the next morning and incubated in 500 μl LB medium with ampicillin. Minipreps were done using Qiagen kits (Qiagen).

Constructs were verified by sequencing using seq1-5 primers (see Table 2.1). Sequencing was performed at the DNA sequencing facility, University of Bergen, using BigDye Terminator v3.1 Cycle Sequencing Kit (Applied Biosystems). Briefly, approximately 200 ng template DNA was mixed with 1 μl BigDye, 1 μl sequencing buffer, 3.2 pmol primer and ddH20 until 10 μl. DNA eluted in TE or Tris was purified and eluted in water for sequencing. PCR conditions were as follows: 96 °C for 5 min, then 25 cycles with 96 °C for 10 sec, 50 °C for 5 sec, 60 °C for 4 min.

Results were analyzed using the Staden sequence analysis package (version 1.7.0) [81].

2.3.2. Subcloning of Shh and Gli1 plasmids

pBluescript-Gli1 [43] and pBluescript-Shh [54] were obtained from Addgene. Plasmids were digested with HindIII and XbaI and subsequently ligated into a HindIII/XbaI-cut pcDNA3.1+ mammalian expression vector (Invitrogen) using T4 ligase (Fermentas).

name	sequence (5' to 3')
numbCloningF-kozak	GCA TCA AGA TCT GCC ACC ATG AAC AAA TTA CGG CAA AGT TTT
numbCloningR	GCA TCA AGA TCT GCA AGT TCA ATT TCA AAC GTC TTC TGT
Numb12-2ndHalfF-fusion	AAG GAA GTT CTT CAA AGG CTT CTT TGG AAA AAC TGG AAA GAA AGC AGT TAA AGC A
Numb12-1stHalfR-fusion	TTT CCA AAG AAG CCT TTG AAG AAC TTC CTT TCA GCT TTC AAT CTT TTT ACA GCA TCT T
seq1 (pCMV)	TTT GAC CTC CAT AGA AGA CAC
seq2 (Numb-specific)	GAA GCG GGA GAA GGA ATG TG
seq3 (Numb-specific)	CTC CGA TGA CCA AAC CAG TG
seq4 (Numb-specific)	CCA CCA GTC CCT TCT TTA AGC
seq5 (GFP)	CAG CAC GAC TTC TTC AAG TC

Table 2.1.: Primers used for cloning and sequencing

2.4. Growth assays

For generation of growth curves, 2.5×10^4 or 5×10^4 cells were plated per well of a 24-well plate in 2.5 ml DMEM. Cell numbers were counted at plating and every 24 hours thereafter for 4 days. For counting, cells were washed once with PBS and 250 μl trypsin were added. Cells were allowed to detach and cell clumps were mechanically dissociated after addition of 250 μl DMEM with 10% FCS. 400 μl of this single cell suspension were counted on a Z2 particle counter (Beckman Coulter). The experiment was performed in triplicates and repeated twice.

For statistical analysis, growth curves were subjected to SPSS exponential curve fitting. The resulting coefficient (k) of the exponential function

$$f(t) = b \cdot e^{k \cdot t}$$

was used to calculate the population doubling time (T).

$$T = \ln 2 / k$$

This was performed for each cell line and each indepent experiment. Means from three experiments were tested for significant differences using Student's t-test.

2.5. Western blotting

Total protein lysates were made using RIPA buffer (Sigma) supplemented with complete mini protease inhibitors (Roche). Cells were lysed in 100 μl lysis buffer per one million cells, transferred to 1.5 ml eppendorf tubes, whisked for 20 sec and sonicated for 30 sec. The lysates were then centrifuged at 10 000 g for 10 min. Supernatants were frozen at $-80\,^{\circ}$C.

Protein amounts were quantified using a BCA assay (Thermo Scientific) compared to a BSA standard according to the manufacturer's instructions. All measurements were performed in duplicates.

10 μg protein was loaded on a 4-12% Bis-Tris NuPAGE gel (Invitrogen) using 4X LDS sample buffer (Invitrogen) and 10% DTT (Invitrogen) in a total volume of 15 μl. Gels were run at 200 V for 50 min in MOPS running buffer (Invitrogen). Gels were blotted at 200 V for 90 min (or at 14 V overnight) onto a nitrocellulose membrane (Amersham) using NuPAGE transfer buffer (Invitrogen). Proper transfer was verified by Ponceau S staining (Sigma).

For all washing steps TBS with 0.5% Tween-20 (Sigma) was used. For blocking, membranes were incubated with 5% skim milk in washing buffer for 1 hour or overnight. All antibody incubations were performed in blocking solution. Each incubation was followed by 3×5 min washing. Primary and secondary antibodies are listed in Table 2.3.

For chemoluminescence detection, blots were incubated with West Pico substrate (Thermo Scientific) for 5 min and imaged using a LAS-3000 unit (FujiFilm) or film. For reblotting, membranes were stripped using Blot Restore (Millipore, Cat.No. 2520) or Restore PLUS (Thermo Scientific).

2.6. Realtime PCR

Total RNA was isolated from cells using RNeasy Plus kit (Qiagen) according to the manufacturer's instructions. RNA was quantified spectrometrically by reading the adsorbance at 260 nm. RNA was transcribed into cDNA using the iScript reverse transcriptase kit (Bio-Rad) according to the manufacturer's instructions. Briefly, 500 ng RNA were used with 2 μl 5X buffer and 0.5 μl enzyme in a 10 μl reaction performed on a thermal cycler (MJ Research). Subsequently, cDNA was diluted in ddH_2O to a total volume of 100 μl. Usually, 1 μl cDNA per reaction was used for realtime PCR.

Realtime PCR was performed on a iCycler unit (Bio-Rad). For a 20 μl reaction, 10 μl 2X SYBRGreen mastermix (Bio-Rad), 4 μl of a 1 μM forward and reverse primer mix and 1 μl template were used. The PCR reaction included 40 cycles of 20 sec denaturation at 95 °C, 20 sec annealing at the temperature stated (see Table 2.2) and 20 sec extension at 72 °C. Melting curve analysis was used to exclude primer-dimer formation and ensure proper amplification. Primer sequences used are listed in Table 2.2.

Results were analyzed using the $\Delta\Delta$Ct-method [73] and normalized to the geometric mean of two housekeeping genes (HPRT1, GAPDH) [86] or to 18S ribosomal RNA. Reactions were performed at least in duplicates.

name	sequence (forward/reverse, 5' to 3')	product size	T_A	reference
numball	ATG CCA AGA AAG CTG AAA CAG AGT CTT CCT CTG CAT AGT GG	284 bp	58	
numb13	CTT CCA AGC TAA TGG CAC TG CTC TTA GAC ACC TCT TCT AAC CA	263 bp	58	
numb24oh2	CAA TCT CCT ACC TTC CAA GGG CGG ACG CTC TTA GAC ACC TC	134 bp	58	
HES1	GCG GAC ATT CTG GAA ATG ACA AGC GCA GCC GTC ATC TG	68 bp	60	[17]
HES5	TGG AGA AGG CCG ACA TCC T GGC GAC GAA GGC TTT GC	65 bp	60	[41]
HPRT1	TGA GGA TTT GGA AAG GGT GT GAG CAC ACA GAG GGC TAC AA	118 bp	58	[74]
GAPDH	GGC ATG GAC TGT GGT CAT GAG TGC ACC ACC AAC TGC TTA GC	87 bp	58	[32]
18S	CGG CTA CCA CAT CCA AGG AA GCT GGA ATT ACC GCG GCT	187 bp	58	[5]

Table 2.2.: Primers used for realtime PCR (T_A: annealing temperature)

2.7. Luciferase reporter assays

For detection Hedgehog signalling activity, a Gli responsive luciferase reporter was used. Its activity correlates with the activation of Gli family transcription factors which are effectors of the pathway. The 8x3'-Gli-BS-luc reporter plasmid was kindly provided by Hiroshi Sasaki (Center for Developmental Biology, Kobe, Japan) [72].

Human U87 glioma cells were co-transfected with 8x-Gli-BS-luc, NUMBx-GFP (or GFP as negative control, respectively) and Shh (or GFP) 24 hours after plating. Transfection was performed using 300 ng reporter plasmid, 300 ng NUMB-M107K (or M107), 300 ng pcDNA-SHH (or pcDNA3.1+), 100 ng β-galactosidase and 3 μl Fugene HD (Roche). After 24 hours, cells were lysed using Reporter Lysis Buffer (Promega). Luciferase activity was determined using Promega Luciferase Assay System (Promega) and normalized to β-galactosidase activity.

2.8. Immunocytochemistry

1×10^4 cells were plated on glass coverslips and allowed to attach overnight. Cells were then washed with PBS and fixed with 4% paraformaldehyde (PFA) (Sigma) for 10 min and

epitope	manufacturer	source	dilution WB	dilution ICC
NUMB	Abcam, ab4147	goat	1:500	1:200
β-Tubulin III	Millipore, MAB1637	mouse	-	1:200
GFAP	Abcam, ab7806	mouse	-	1:500
p53	Santa Cruz, sc-126	mouse	1:100	-
GFP	Millipore, AB3080	rabbit	1:500	-
Ki67	Dako, M7240	mouse	-	1:200
pHistone H3	Abcam, ab47297	rabbit	-	1:2000
Actin	MP Biomedicals, clone C4	mouse	1:5000	-
anti-Goat HRP	Santa Cruz, sc-2768	rabbit	1:25,000	-
anti-Goat HRP	Santa Cruz, sc-2953	chicken	1:25,000	-
anti-Mouse HRP	Santa Cruz, sc-2005	goat	1:25,000	-
anti-Mouse Cy3	Zymed	goat	-	1:200
anti-Goat, biotinylated	Vector Labs, BA-9500	horse	-	1:100
anti-Mouse Alexa 647	Invitrogen, A21236	goat	-	1:1000
anti-Rabbit Alexa 647	Invitrogen, A21244	goat	-	1:1000

Table 2.3.: Antibodies used for western blotting and stainings

permeabilized for 4 min in 0.5% Triton-X 100 (Sigma) in PBS. A 0.1% Triton-X/PBS solution was used as washing buffer and solvent for all subsequent steps. After washing, cells were blocked in 5% serum from the secondary antibody species for 15 min. Primary antibodies (see Table 2.3) were incubated for 45 min at 37 °C followed by washing in PBS for 2×5 min. Secondary antibodies were incubated for 45 min at 37 °C followed by washing in PBS for 3×5 min. For biotinylated secondary antibodies, an Extravidin-Cy3 conjugate (Sigma, 1:200) was used as fluorochrome.

Finally, coverslips were mounted on glass slides using ProLong mounting medium with DAPI (Invitrogen). Imaging was performed at the Molecular Imaging Center (Fuge, Norwegian Research Council), University of Bergen, on a Nikon TE2000 flourescence microscope (Nikon) or a Meta 510 confocal laser scanning microscope (Zeiss). Additional imaging was performed using an Axiovert 135 fluorescence microscope (Zeiss).

2.9. Flow cytometry

Flow cytometry was performed on a FACSCalibur cytometer (BD Biosciences) using CellQuest Pro software. Forward and sideward scatter photomultiplier (PMT) voltages were

optimized for the main cell population. A gate was drawn around this population to exclude cell debris and cell clumps. This gate was applied to all further dot plots and histograms used for analysis. For green fluorescence detection, the FL1 channel was used in logarithmic mode.

2.10. Virus production

2.10.1. Production

Lentiviral particles were packaged in HEK293T cells. 2.5 million cells were seeded in 10cm dishes. The following day, cells were transfected using 5 μg total DNA and 15 μl Fugene HD (Roche) after 15 min incubation. The complex was added dropwise to the cells. 24 hours later, medium was replaced by DMEM with 30 % FCS.

Viral supernatants were harvested twice, on day 2 and day 3 after infection. Supernatants were filtered through 0.45 μm AeroDisc syringe filters (Pall Corporation) to remove cells and cell debris, aliquoted and stored at −80 °C or at 4 °C until concentration.

For serum-free supernatants, the protocol was modified as proposed by *Sena-Esteves et al.* [75]. OptiMEM (Invitrogen) was used for harvest instead of high serum DMEM. Before addition of harvesting medium, cells were washed twice with 10 ml plain DMEM, then 8 ml OptiMEM were added.

2.10.2. Ultracentrifugation

Sterile ultracentrifuge tubes (38.5 ml straight wall, ultra thin, Beckman Coulter) were filled with 32 ml supernatant. A 30 % solution of sucrose was prepared in PBS and sterile-filtered. Then, supernatants were underlaid with a 5 ml sucrose cushion. Care was taken not to introduce air bubbles by taking up 7 ml sucrose using 5 ml pipettes and discarding the remaining 2 ml.

The filled tubes were transferred to buckets of a SW-28 rotor (Beckman Coulter) and corresponding pairs were weighed. No more than 100 mg weight difference was allowed. Any differences were corrected by addition of plain DMEM. Supernatants were then centrifuged at 26 000 rpm for 2 h at 4 °C in an ultracentrifuge (Beckman Coulter). After spinning, supernatants were decanted and the inverted tube was shortly air-dried in a laminar flow hood.

Finally, the pellet was resuspended in an appropriate amount of PBS or OptiMEM. Usually, 1/100 of the initial volume was used. The pellet was allowed at least 6 h at 4 °C with shaking or agitation to completely dissolve. Concentrated virus was aliquoted and stored at −80 °C.

2.10.3. Titration

5×10^4 U87 cells were plated in 1 ml complete DMEM per well of a 24-well plate and incubated overnight. Duplicate wells were plated per virus and dilution step and a negative control for flow cytometry was added.

The following day, appropriate dilutions of the viral supernatants to be tested were added to each well in a total volume of 1 ml complete DMEM with $8\,\mu g\,\mu l^{-1}$ polybrene (Sigma). Wherever possible, plates were centrifuged at 2250 rpm for 90 min at 31 °C to increase transduction efficiency. The next day, growth medium was replaced by 1 ml complete DMEM. Two to three days after transduction, cells were washed once with PBS and trypsinized. A single cell suspension was achieved by brief pipetting. Cells were then fixed for 15 min in 4% PFA at room temperature and washed with PBS. V-bottom 96-well plates (Nunclon, Thermo Fisher Scientific, Waltham, MA, USA (Thermo Scientific)) were used to facilitate handling of large numbers of samples.

Transduction efficiency was analyzed by flow cytometry. The percentage of GFP positive cells was determined in comparison with wildtype control. Transduction by only one virus particle was assumed when the percentage of GFP+ cells was between 5% and 20%. Appropriate samples were selected for calculation of virus titer by the formula:

$$\text{titer [TU/ml]} = \frac{\text{GFP\%} \cdot \text{seeded cells}}{\text{total infection volume} \cdot \text{dilution factor} \cdot 100}$$

2.11. Animal experiments

All animal experiments were performed with the approval of and in accordance with the recommendations laid down by the Norwegian State Commission for Laboratory Animals (Forsøksdyrutvalget, Saks-Nr. 08/86800-2008300). Nude rats (rnu/rnu) were received from an in-house breeding facility. Prior to all experiments, rats were allowed one week for acclimatization. Wherever possible, animals were housed in pairs and marked by ear-clipping.

2.11.1. Intracranial tumor implantation

Nude rats were anesthetized by subcutaneous injection of medetomidine (Orion Pharma) and ketamine (Pfizer). Anesthetized animals were fixed in a stereotactical frame. The operation site was desinfected using 70% ethanol and animals received a 0.5 ml s.c. injection of bupivacaine 0.5% into the scalp as local anesthesia. After 5 min, a longitudinal incision was made. Skull sutures were exposed by blunt preparation.

A drill hole was made 3 mm right of the sagittal suture and 1mm posterior of the bregma. Meninges were incised with an eye scalpel to facilitate entry of the injection needle. Using a Hamilton syringe (Hamilton), 5×10^4 cells were injected 2.5 mm beneath the dura. Finally, the wound was closed by suture.

After surgery, rats were allowed to recover from anesthesia in a prewarmed incubator.

2.11.2. Magnetic resonance imaging

Animals were followed up by weekly MRI. Rats were anesthetized using isoflurane (Schering-Plough) inhalation and respiratory function was monitored during the procedure. T2 weighted sequences were acquired on a 7 Tesla animal scanner (Bruker).

2.11.3. Survival analysis

Animals were euthanized by CO_2 inhalation when clinical symptoms (e.g. slowing down of motoric functions, disturbance of equilibrium) arose or intolerable tumor size was determined by MRI.
Survival times were visualized using Kaplan-Meier graphs and significant differences were detected by pairwise comparison of treatments using Log-rank tests.

2.11.4. Immunohistochemistry

Fixed-frozen sections After euthanization and preparation of the thoracic cavity, rats were perfused through the left ventricle with saline until the liver appeared pale and then perfused with 4% PFA. Brains were excised and stored in PFA overnight. The next day, brains were transferred into a 30% sucrose solution in a 50 ml tube. They were allowed to sink to the bottom of the tube (which took approximately 3 days). Brains were covered with TissueTek OCT compound (Sakura) and immersed in isopentane that had been prechilled using dry ice. Then they were stored at −80 °C.

Rat brains were cut into 12 μm sections on a cryostat (Leica) and stored at −80 °C until staining.

H&E staining For H&E staining, frozen sections were dehydratated by immersion in acetone for 10 minutes, followed by 7 min treatment in chloroform. Slides were then allowed to dry for 15 min. Sections were then stained in hematoxylin for 10 min, rinsed with tap water and washed with destilled water, before exposure to eosine for 1 min. Next, sections were washed in destilled water, immersed in increasing concentrations of ethanol (70%, 96%, 100%) and finally put into xylol for 10 min.

Fluorescence microscopy For visualization of GFP fusion proteins, fixed-frozen sections were allowed to warm to room temperature for 20 min. They were then fixed in 4% PFA for 15 min, washed in phosphate buffered saline (PBS) and mounted using ProLong Gold with DAPI (Invitrogen) for staining of nuclei.

2.12. Microarray data and analysis

Published microarray data from Lee et al. [47] (Accession number GSE4536) were retrieved from a public repository (GEO and ArrayExpress). Preprocessed data were annotated and log2-transformed. Hierarchical clustering and t-tests were performed using MultiExperiment Viewer v4.6 [68] and Cluster 3.0/TreeView [24].

2.13. Statistics

All statistical tests were performed using SPSS Statistics 17 (SPSS). P-values smaller than 0.05 were considered statistically significant.

3. Results

3.1. NUMB expression in patient material

NUMB mRNA levels were determined in a small panel of biopsy material from tumors that were histologically confirmed GBMs. As a reference, nonneoplastic brain tissue was used (Figure 3.1). NUMB was detected at various levels in normal brain and in all tumor samples.

Next, NUMB protein expression was determined by western blotting in biopsy samples and commercially available normal human brain samples (Figure 3.2). Expression of NUMB was seen in all samples, and NUMB2 (66 kD) or NUMB4 (65 kD) isoforms were expressed at much higher levels than NUMB1 (72 kD) or NUMB3 (71 kD).

For patient samples P22, P35 and P38, which were examined both by realtime PCR and western blotting, mRNA levels correlated roughly with protein levels.

3.2. Differential expression of NUMB isoforms in adherent glioma cell lines

NUMB mRNA levels were determined in glioma cell lines by use of isoform-specific primers. Because of the alternative splicing of two non-neighbouring exons, expression levels cannot be measured for each isoform separately. However, primer pairs either detecting NUMB2+4 or NUMB1+3 isoforms were successfully designed. Additionally, primers detecting all four isoforms were used. Isoform specific primers were designed to bind on exon-exon junctions unique to the isoforms to be detected.

Using plasmids carrying either NUMB3 or NUMB4 coding sequences, it could be shown that these assays can indeed distinguish these two pairs of isoforms depending on alternative splicing in their proline-rich region.

For NUMB1/3 primers, copy numbers of NUMB3 could be reliably quantified over a dynamic range of four orders of magnitude without being disturbed by addition of up to 10^6 copies of NUMB4 (Figure 3.3, left panel). The same was true for NUMB2/4 primers using an analogous experiment design (Figure 3.3, center panel). The squared correlation coefficients were $R^2 = .993$ for the NUMB1/3 realtime PCR, and $R^2 = .991$ for the

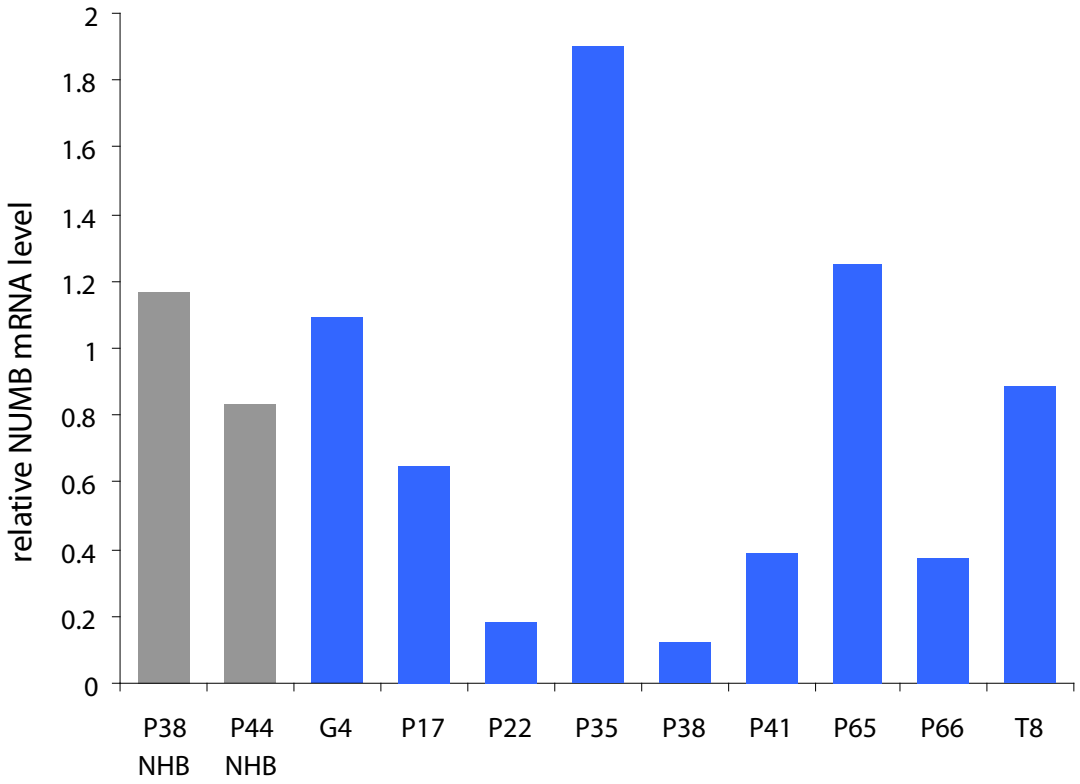

Figure 3.1.: **NUMB mRNA levels in GBM biopsies.** Total NUMB levels were determined by realtime PCR in patient samples (*blue bars*). Nonneoplastic surgical brain material (*grey bars*) was used as a reference (NHB = normal human brain). Values were normalized to 18S ribosomal RNA.

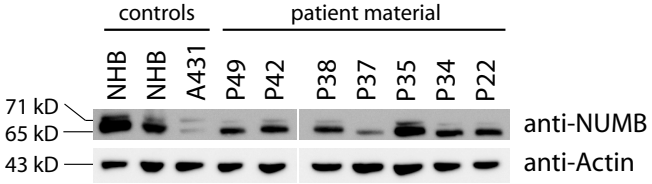

Figure 3.2.: **NUMB protein levels in GBM biopsies.** NUMB expression was determined by western blotting. Commercial normal human brain (NHB) samples serve as a reference. The epidermoid carcinoma cell line A431 was included to illustrate the two bands detected by the antibody, corresponding to 65/66 kD and 71/72 kD isoforms, respectively. Actin was used as loading control.

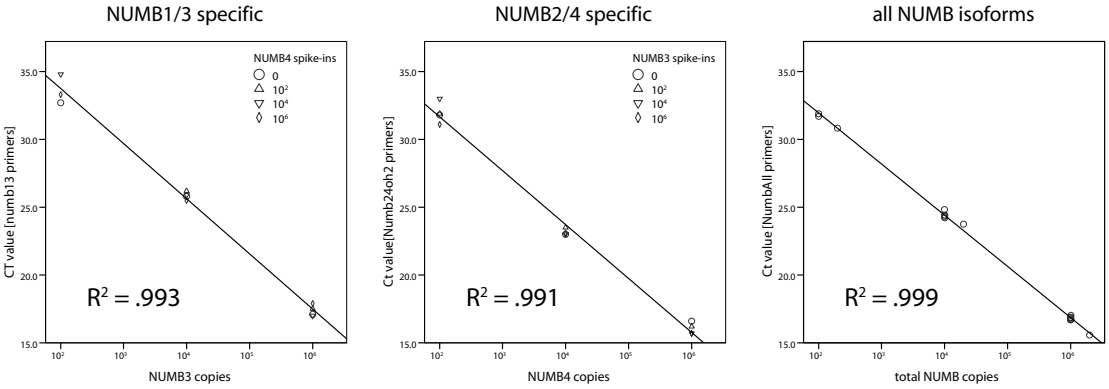

Figure 3.3.: **Linearity of isoform specific realtime PCR** Up to 10^6 copies NUMB4 cDNA were spiked with up to 10^6 copies of NUMB3 cDNA and detected by realtime PCR with primers specific for either NUMB1/3 (*left*), NUMB2/4 (*center*) or all isoforms (*right*). Squared Pearson's correlation coefficient R^2 is shown as measure of linearity.

NUMB2/4 assay. A third pair of primers detects both plasmids at similar sensitivity and linearity ($R^2 = .999$) (Figure 3.3, right panel).

Expression levels were then determined in a set of glioma cell lines. All cells examined expressed NUMB, but NUMB2/4 levels were more than 100fold higher than NUMB1/3 levels (Figure 3.4), assuming equal PCR effiencies.

3.3. Generation of NUMB lentiviral vectors

To study effects of NUMB on glioma cells, lentiviral vectors containing the coding sequence of human NUMB isoforms fused in-frame to enhanced green fluorescent protein (eGFP) under the control of the cytomegaly virus (CMV) promoter were cloned (Figure 3.5). For plasmid maps, please refer to the appendix (Figure A.1).

NUMB coding sequences for each of the four human isoforms were either extracted directly from total RNA or subcloned from plasmids from other laboratories. To facilitate virus titration and subcellular localization, eGFP fusion proteins were generated. The transgene was put under control of the CMV promoter whose excellent transcriptional activity enables high expression levels. A Kozak consensus sequence was introduced before the NUMB start codon in order to enhance translation.

Lentiviral vectors were chosen because of their ability to infect both dividing and non-dividing cells with high efficiency. Viral particles were pseudotyped with the vesicular

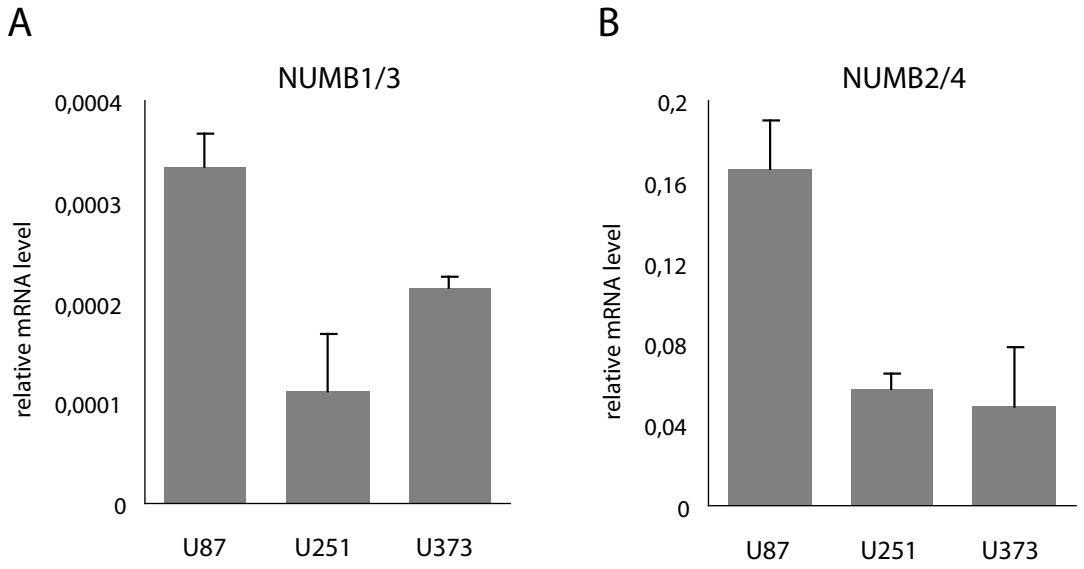

Figure 3.4.: **mRNA levels of NUMB isoforms in adherent glioma cell lines** Gene expression levels of (A) NUMB1/3 or (B) NUMB2/4 isoforms were measured by realtime PCR in U87-gfp, U251-gfp and U373-gfp cells. Values are relative to the geometric mean of GAPDH and HPRT1 housekeeping genes. Error bars indicate standard deviation. Note different scaling of the two panels.

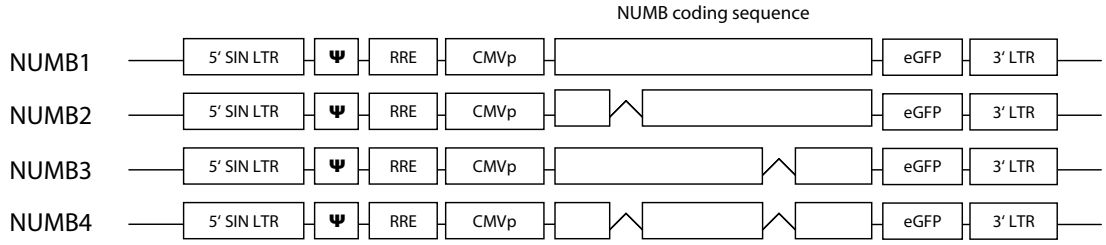

Figure 3.5.: **NUMB lentiviral vectors** NUMB coding sequences were fused to eGFP under control of the CMV promoter. Alternative splicing of the four different human isoforms is indicated. Viral elements include self-inactivating (*SIN*) long terminal repeats (*LTR*), ψ packaging signal (ψ) and rev-responsive element (*RRE*). The drawing does not reflect proportional length of nucleotide sequences.

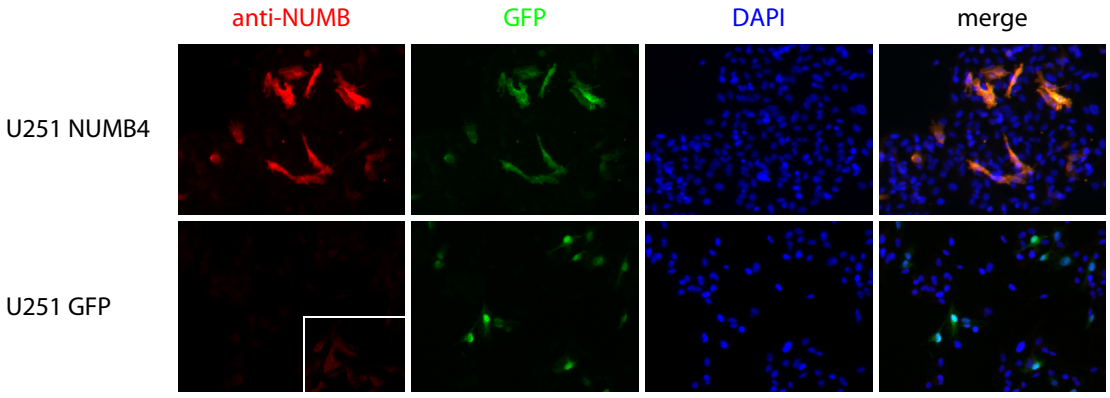

Figure 3.6.: **Verification of NUMB-GFP fusion proteins** Immunocytochemical staining of U251 cells transduced with either NUMB4-GFP or GFP alone as negative control. NUMB stainings were imaged with optimal exposure for exogenous NUMB, making endogenous levels hard to identify. However, increased contrast shows proper detection of basal NUMB levels as well (*insert, lower panel*). Nuclei are stained with DAPI.

stomatitis virus G protein (VSV-G) which equips the virus with a broad tropism for mammalian cells.

Viral supernatants were produced in 293T cells (batches of virus and corresponding titers are summarized in Supplementary Table A.1). Colocalization of NUMB and GFP was verified by immunostaining of infected cells. A clear overlap of NUMB immunoreactivity and GFP fluorescence was found (Figure 3.6).

3.4. Generation of U87-NUMB cell lines

Using lentiviral infection, human U87 glioma cell lines were generated to stably overexpress the NUMB isoforms which supposedly account for differentiation of neural progenitor cells during mammalian development, i.e. NUMB2 and NUMB4. Cells were infected at a multiplicity of infection (MOI) ranging from 5 to 10. Expression of the transgene was verified by western blotting (Figure 3.7). Protein bands at 65/66 kD and 71/72 kD show endogenous NUMB levels which were unchanged by NUMB overexpression. Ectopic NUMB-gfp was detected at about 90 kD and at high levels. Both wildtype cells and cells overexpressing GFP only served as controls.

Transduction effiency was determined using flow cytometry. Transduction rates were 81.5% for U87-NUMB2, 88.3% for U87-NUMB4 and 99.8% for U87-gfp (Figure 3.8). Interestingly, NUMB overexpressing cells showed two distinct populations: one being highly GFP positive, the other one expressing NUMB-gfp at a very low level. Even though part of

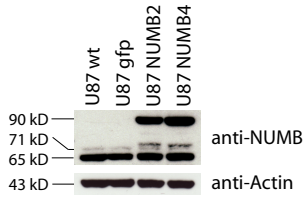

Figure 3.7.: **NUMB protein levels in stably transduced human U87 glioma cells.** Anti-NUMB western blots of U87 cells overexpressing NUMB2-GFP, NUMB4-GFP, GFP or wildtype cells.

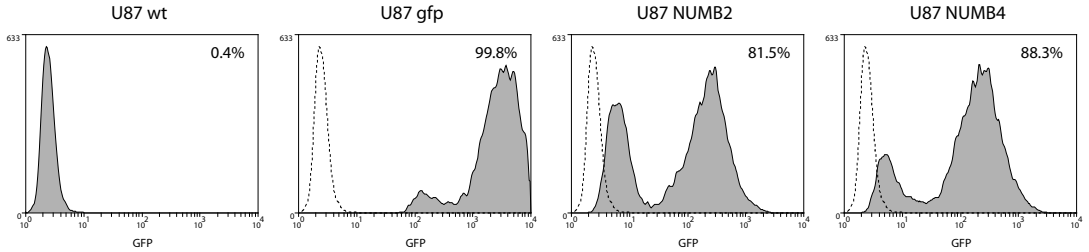

Figure 3.8.: **Transduction efficiency of stably transduced human U87 glioma cells.** After transduction with lentiviral particles, fluorescence of NUMB-gfp fusion proteins was used to determine transduction efficiency by flow cytometry. Percentages were determined by gating just above the wildtype peak.

this population was outside the gate by which the rate of GFP+ cells was calculated, it seemed that almost all of these cells express the transgene because the mean fluorescence level is above that of wildtype cells.

3.5. Unchanged proliferation in cell culture

Growth curves of U87 NUMB overexpressing cell lines were generated in order to compare proliferation in cell culture (Figure 3.9). No significant differences with respect to growth rate were found based upon the calculated population doubling times (Table 3.1).

To test whether proliferation was specifically inhibited in transduced cells, we examined Ki67 expression, which labels all cells but those in G0 phase, i.e. cycling cells. In U251 cells transduced with NUMB4 at low MOI (less than 1), transduced cells continued to express Ki67, indicating that proliferation is not blocked by overexpression of NUMB (Figure 3.10A).

Similarily, we analyzed expression of phosphorylated histone H3, which is selectively expressed in cells during M phase. In wildtype and gfp controls as well as NUMB2 or NUMB4 overexpressing U87 cells, a low percentage of mitotic cells could be detected (Figure 3.10B).

cell line	**population doubling time** (hours ± SD)	***p*-value**
U87 wt	29.30 ± 0.72	-
U87 gfp	30.75 ± 2.72	.099
U87 NUMB2	31.63 ± 2.38	.056
U87 NUMB4	29.79 ± 1.91	.206

Table 3.1.: **Proliferation of NUMB transduced U87 cells** Growth rates were determined from the corresponding growth curves by curve fitting. Population doubling time was then calculated (SD = standard deviation). Student's t-test was used to test for significant differences compared to wildtype cells. Means from three independent experiments are shown.

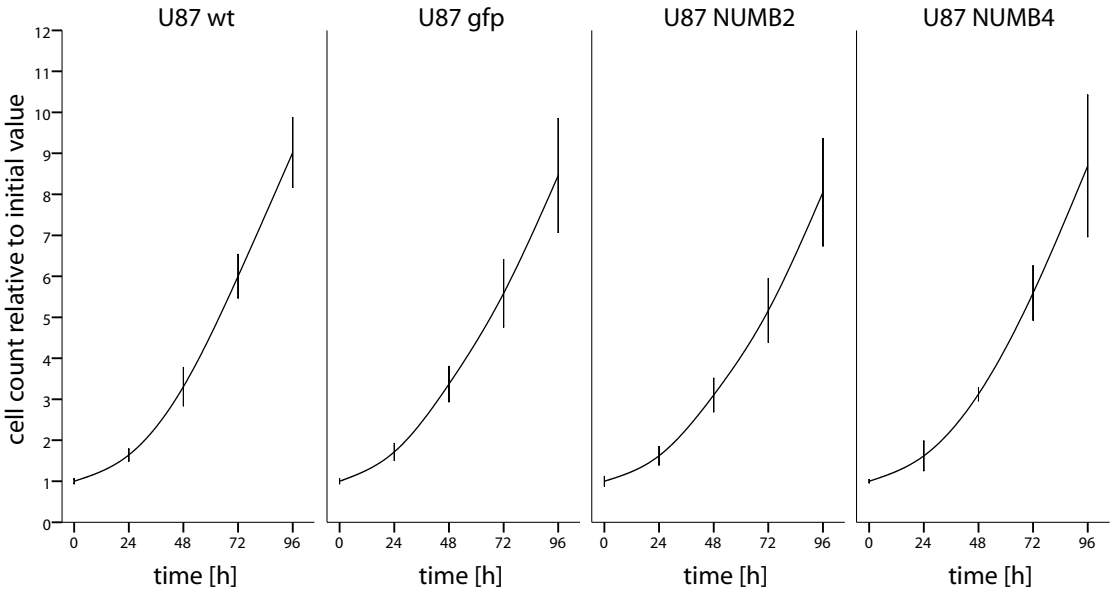

Figure 3.9.: **Growth curve of U87 stably transduced cells.** Different U87 cell lines were plated in 24-well plates. Cells were trypsinized daily and counted using an automatic particle counter. Means from three independent experiments are shown. Error bars indicate standard deviation.

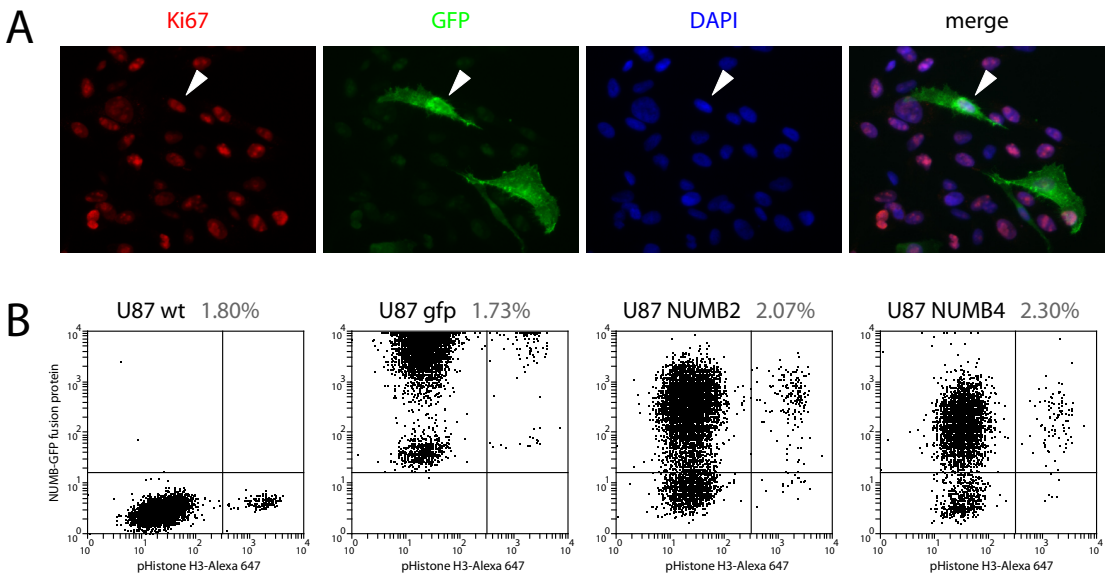

Figure 3.10.: **NUMB overexpression does not cause cell cycle arrest.** (*A*) U251 cells virally transduced with NUMB4-gfp (*green*) were stained immunocytochemically for Ki67 (*red*). Nuclei were stained with DAPI (*blue*). (*B*) A single cell suspension of U87 cells stably expressing NUMB2-gfp, NUMB4-gfp or gfp alone were stained for phospho-Histone H3 and analyzed by flow cytometry. The percentage of phospho-Histone H3 positive cells is indicated.

There was no dramatic increase or decrease in the M phase fraction that could indicate cell cycle arrest.

3.6. No induction of differentiation by NUMB in U87

It was then examined whether overexpression of NUMB would induce differentiation of U87 cells. There was no alteration in morphology in NUMB2 or NUMB4 transduced cells compared to wildtype or GFP controls (Figure 3.11). U87 cells are variously shaped, but characterized by multiple processes. This appearance was preserved in NUMB overexpressing cells.

In order to more accurately identify differentiated cells, expression of the glial marker GFAP and the neuronal marker β-Tubulin III was determined by immunocytochemical staining. A weak basal level of β-Tubulin III expression was present in all samples, but no increase could be shown by overexpression of NUMB2 or NUMB4 (Figure 3.12, *upper panel*). Likewise, almost no expression of GFAP could be observed in controls or in NUMB

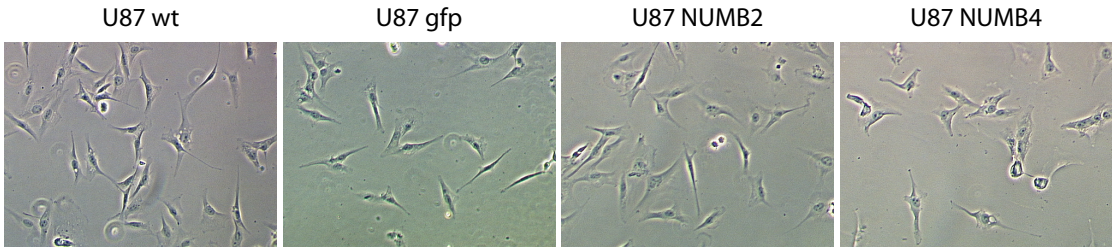

Figure 3.11.: **Morphology of U87 stably transduced cells.** Bright field microscopy images of U87 cells overexpressing NUMB2-GFP, NUMB4-GFP or GFP were compared to wildtype cells.

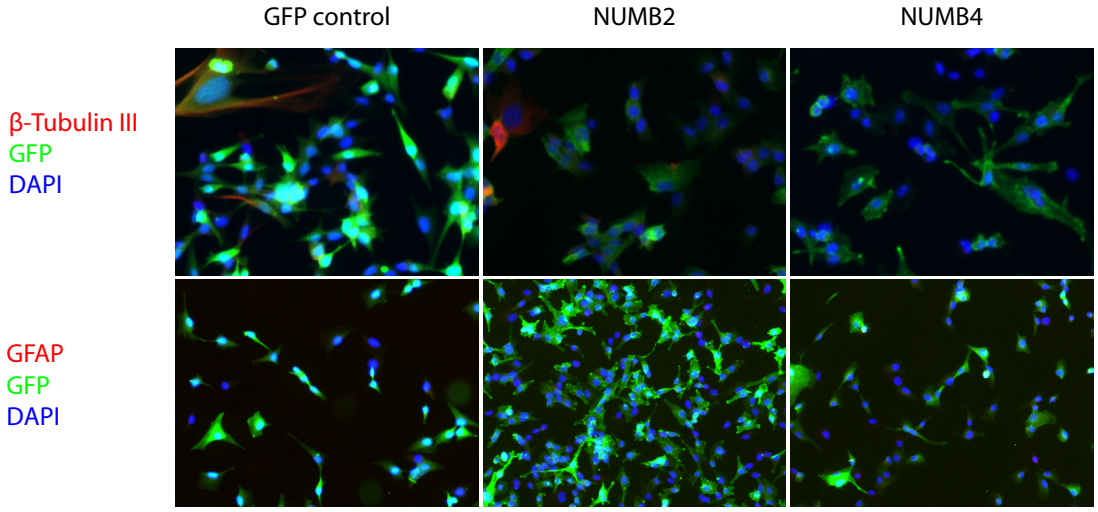

Figure 3.12.: **Staining of glial and neuronal markers in U87 stably transduced cells.** U87 cells overexpressing NUMB2-GFP, NUMB4-GFP or GFP alone as negative control were stained with antibodies against β-tubulin III or GFAP (*red*). Nuclei were stained with DAPI (*blue*) while NUMB expression is visualized by GFP fusion proteins (*green*).

overexpressing cells (Figure 3.12, *lower panel*). Very few single positive cells were detected in all stainings and served as internal positive controls.

3.7. NUMB transduced U87 cells are tumorigenic in vivo

Orthotopic xenografts of U87-gfp, U87-NUMB2-gfp and U87-NUMB4-gfp cells were established in nude rats to test if these cells could generate tumors and to characterize their morphology in vivo by MRI and histology. Furthermore, survival time until the onset of clinical symptoms was compared. This pilot experiment included three animals per group. One animal died one day after surgery and was excluded from the analysis.

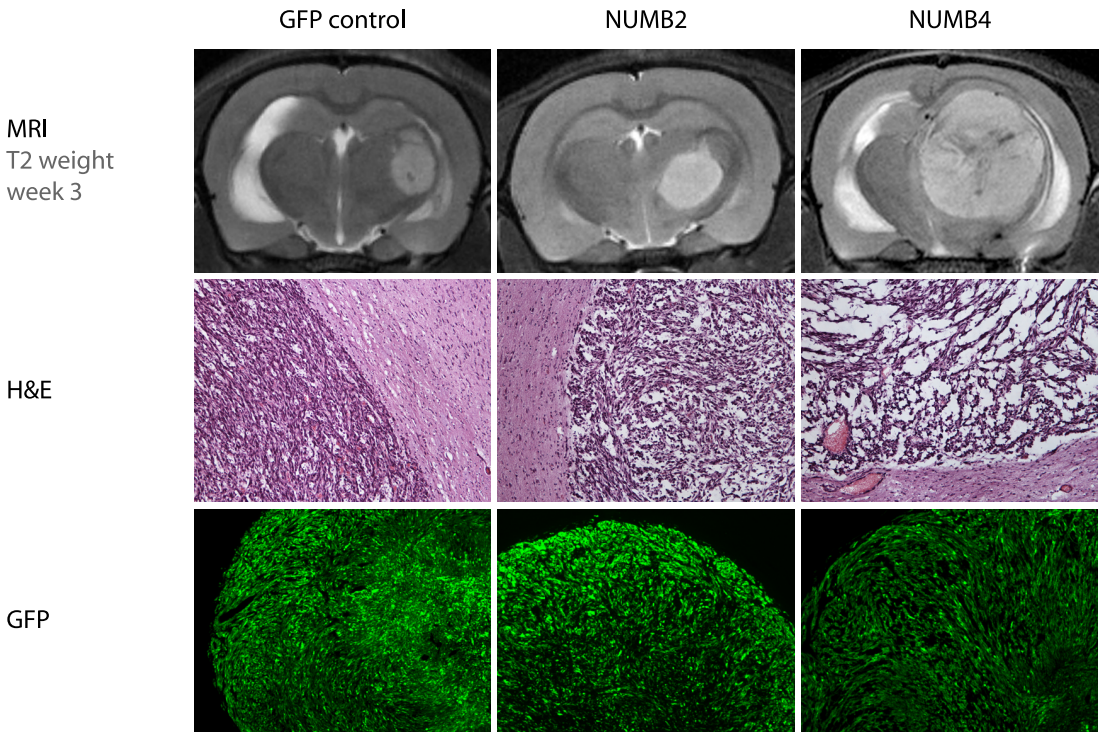

Figure 3.13.: **Xenografts of U87-NUMB cells.** T2-weighted MRI images from week 3 after tumor implantation are shown, as well as H&E stainings and immunofluorescence images of a representative tumor of each group.

Tumorigenicity All three cell lines were able to generate tumors in vivo with 100% tumor take (Table 3.2), indicating that overexpression of NUMB2 or NUMB4 does not block engraftment. Histological sections also showed that the tumors indeed consist of GFP positive cells (Figure 3.13, *bottom panel*), i.e. there is no outgrowth of transduced cells by untransduced wildtype cells.

Morphology Tumor growth was followed up by weekly MRI. Tumors from all groups could be clearly identified in T2 weighted images (Figure 3.13, *top panel*). The lesions seen on MRI were clearly circumscribed in all groups.

Analysis of histological morphology showed typical features of U87 xenografts, i.e. a clearly demarkated tumor mass (Figure 3.13, *middle panel*). The high density of cells seen in GFP controls, however, was loosened up in NUMB2 and especially NUMB4 tumors due to a pseudocystic tumor matrix.

cell line	tumor take	survival (days ± SD)	*p*-value
U87 gfp	3 / 3	29.0 ± 2.0	-
U87 NUMB2	3 / 3	27.7 ± 2.5	.486
U87 NUMB4	2 / 2	23.5 ± 3.5	.039

Table 3.2.: **Tumor take and survival in U87 xenografted animals** For each group, the tumor take is shown along with the mean survival (*SD* = standard deviation). Indicated p-Values are from log rank tests of NUMB2 or NUMB4 survival data compared to gfp controls. One NUMB4 animal was lost briefly after surgery and was excluded from the analysis.

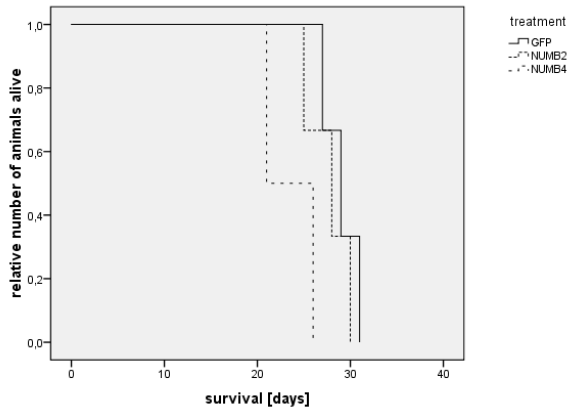

Figure 3.14.: **Kaplan-Meier graphs of survival of animals bearing U87 xenografts.** Animals bearing U87-NUMB2, U87-NUMB4 or U87-gfp tumors were euthanized upon arousal of clinical symptoms.

Survival Finally, analysis of survival showed that animals bearing NUMB4 tumors had a shorter survival time than GFP controls or animals with U87-NUMB2 (Figure 3.14). This result was found statistically significant, but care should be taken regarding the small numbers per group (Table 3.2).

3.8. Regulation of signalling pathways by NUMB in adherent glioma cell lines

After characterization of growth kinetics of NUMB overexpressing tumors in vitro and in vivo, we investigated if functional pathway interactions described in literature could also be found in glioma cell lines. These experiments were performed in different adherent glioma cell lines expressing ectopic NUMB by either transfection or viral transduction.

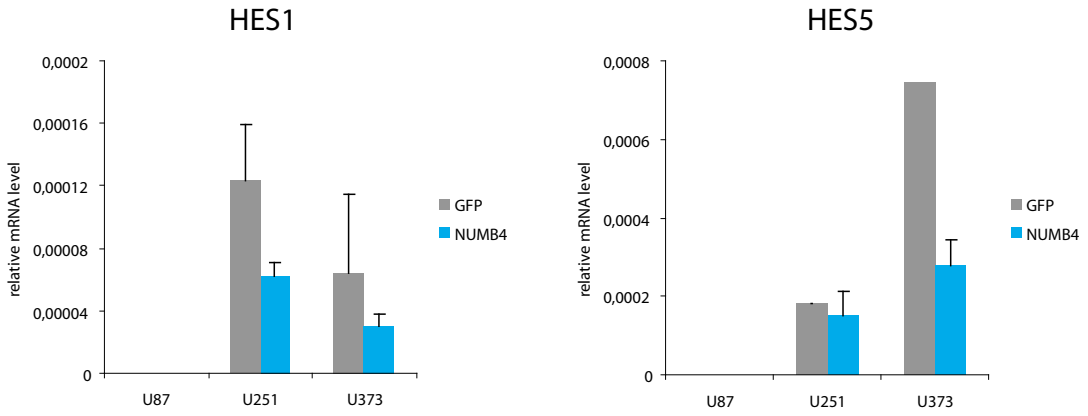

Figure 3.15.: **Downregulation of NOTCH signalling by NUMB overexpression** HES1 and HES5 mRNA levels were detected by realtime PCR. Cells were transduced with NUMB4-GFP or GFP alone at low MOI. Values are normalized by the geometric mean of HPRT1 and GAPDH housekeeping genes. Error bars indicate standard deviation.

Notch signalling By examining gene expression levels of HES1 and HES5 transcription factors which are effectors of the Notch signalling pathway, we aimed to determine whether NUMB overexpression can inhibit Notch activity in vitro. Approximately 2-fold downregulation of HES1 could be shown in U251 and U373 cells by overexpression of NUMB4. HES5 levels were inconsistent, but a trend towards downregulation was seen. In U87 cells however, endogenous HES1 and HES5 levels were below the detection limit of the PCR, so regulation of the pathway could not be assayed (Figure 3.15).

Hedgehog signalling Activity of the Hedgehog signalling pathway was determined by a luciferase reporter gene assay detecting changes in expression of the GLI family of transcription factors. In humans, GLI1 through GLI3 are effectors of Hedgehog signalling.

In order to show modulation of Hedgehog signalling by NUMB, the pathway was stimulated by overexpression of the SHH ligand (Figure 3.16A). Moderate increase in Hedgehog activity was seen. However, no attenuation of GLI activity by NUMB overexpression was observed.

As a reference, human embryonic kidney cells (293T) which can reportedly be stimulated by SHH [53] were used. Here, only moderate induction was seen, too (Figure 3.16B). Finally, to insure that the assay could be induced at all, U87 cells were co-transfected with reporters and GLI1, which directly induces transcription of the luciferase construct. Here, about 40fold inducted was seen (Figure 3.16C).

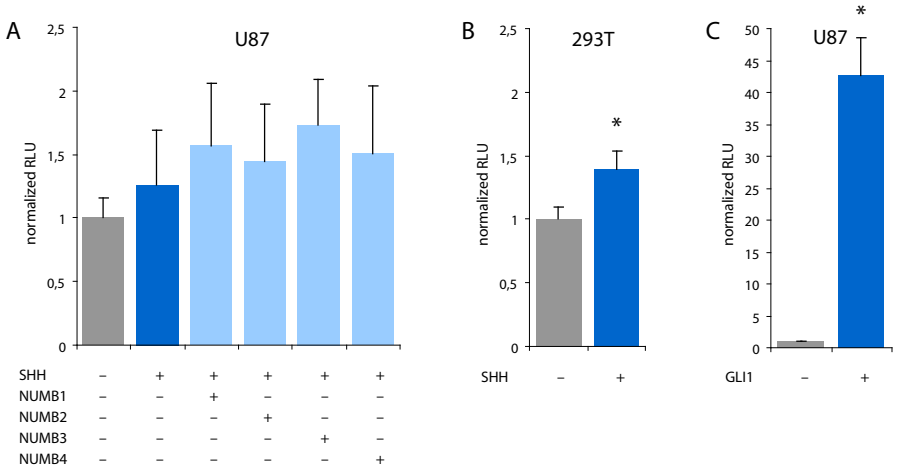

Figure 3.16.: **Modulation of Hedgehog signalling by NUMB** Quantification of Hedgehog signalling activity by GLI-responsive luciferase reporter gene assay. Cells were transfected with a luciferase reporter plasmid and a β-galactosidase plasmid for normalization. (A) U87 cells were co-transfected with SHH (or vector control) and NUMB isoforms (or vector control). (B) 293T cells stimulated by SHH co-transfection and (C) U87 cells stimulated by GLI1 co-transfection served as positive controls. All values are normalized to β-galactosidase activity and relative to baseline levels. Measurements were performed in duplicates and means from three transfections are shown. Asterisk (*) indicates $p < 0.05$.

p53 Western blotting of p53 showed no differential expression in U87 cells transduced with NUMB compared to wild type and GFP cells (Figure 3.17).

3.9. NUMB expression in gliomaspheres

In order to explore differential expression of NUMB in cancer stem cells and other cancer cells, published microarray data from Lee et al. [47] were reevaluated with respect to expression of NUMB related genes.

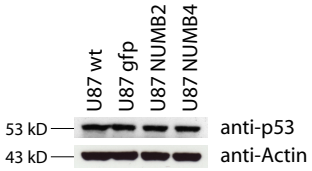

Figure 3.17.: **p53 protein levels in NUMB transduced U87 cells.** Lysates from cell lines overexpressing NUMB2 or NUMB4 and corresponding controls were probed with anti-p53 antibody. Actin was used as loading control.

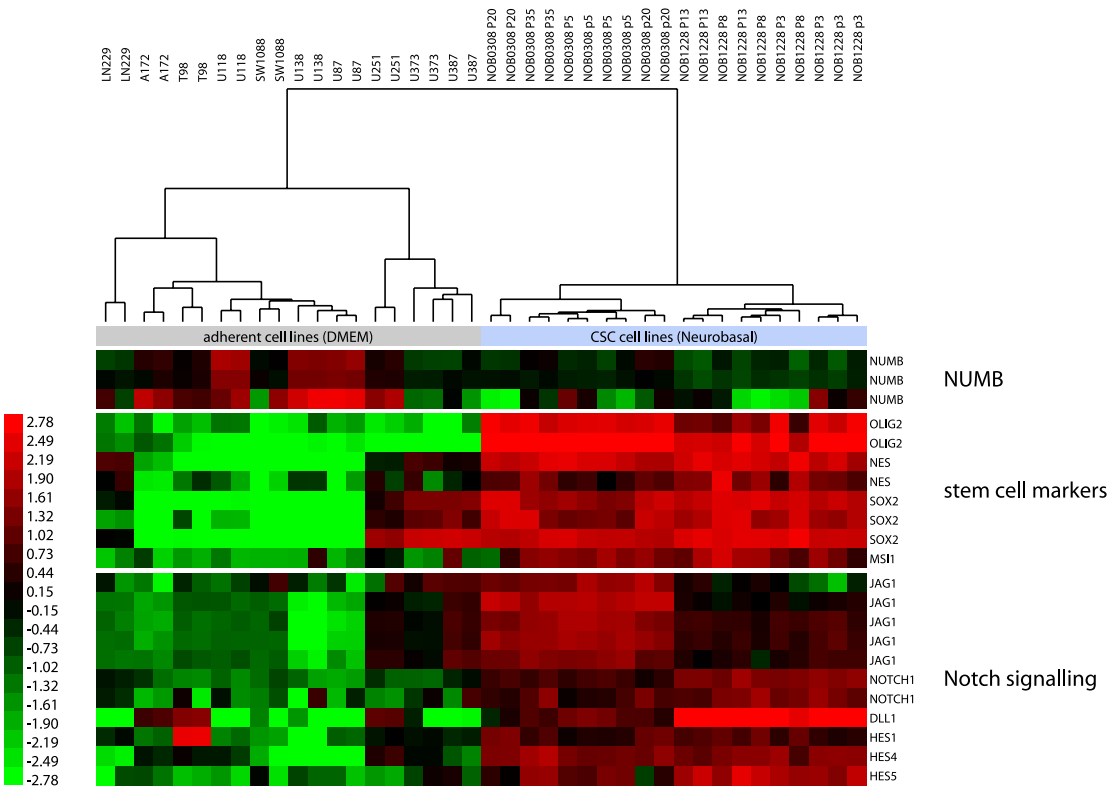

Figure 3.18.: **Expression of NUMB related genes in microarray data from *Lee et al. 2006*.** Normalized microarray data were retrieved from a public repository, log2-transformed and subjected to hierarchical clustering. Only genes that are differentially expressed (t-Test) between CSC and DMEM cells are shown. Multiple rows from the same gene indicate different probes. Intensities are color-coded from low (*green*) over medium (*black*) to high (*red*).

Hierarchical clustering reliably distinguished between traditional adherent glioma cell lines grown in DMEM with FCS from cell lines grown as neurospheres in NSC medium with a stem-cell phenotype. Expression levels of NUMB and those of frequently used stem cell markers (SOX2, MSI1, OLIG2) and Notch signalling related genes were inversely correlated and differentially expressed in serum cell lines and gliomaspheres (Figure 3.18).

We then examined NUMB expression on the protein level in gliomaspheres and compared to adherent glioma cell lines grown in DMEM with FCS. For this experiment, we used a small panel of glioma cell lines established in NSC medium (kindly provided by Katrin Lamszus, Hamburg). Even though derived under the same conditions, some of them appear as free-floating neurospheres while others grow adherently or semiadherently as spheroids attached to the culture flasks [31].

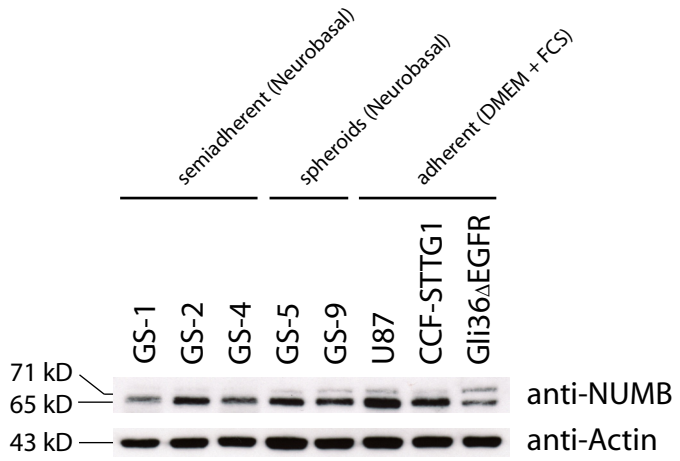

Figure 3.19.: **NUMB expression in gliomaspheres and adherent glioma cell lines.** NUMB expression in a small panel of glioma cell lines grown in neural stem cell medium (GS-1 to GS-9), compared to adherent glioma cell lines grown in serum-containing DMEM (U87, CCF-STTG1, Gli36ΔEGFR). Actin was used as loading control.

Western blotting shows that NUMB expression was higher in U87 than any other cell line examined (Figure 3.19). Expression in neurospheres was lower, but no differences could be seen between gliomaspheres and the semiadherent cells grown in Neurobasal medium.

3.10. NUMB does not change morphology of cancer stem-like glioma cells

Finally, all four human NUMB isoforms were overexpressed in GS-5 and GS-9 gliomaspheres because of lower endogenous NUMB levels and their well documented stem-like properties.

Neurospheres were infected with lentiviral particles right after dissociation. 48 hours after infection, cells had reaggregated or started to form new spheroids irrespective of NUMB overexpression (Figure 3.20). Cells were followed up until 5 weeks after infection and were regularily dissociated for passaging but no changes in morphology could be observed (data not shown).

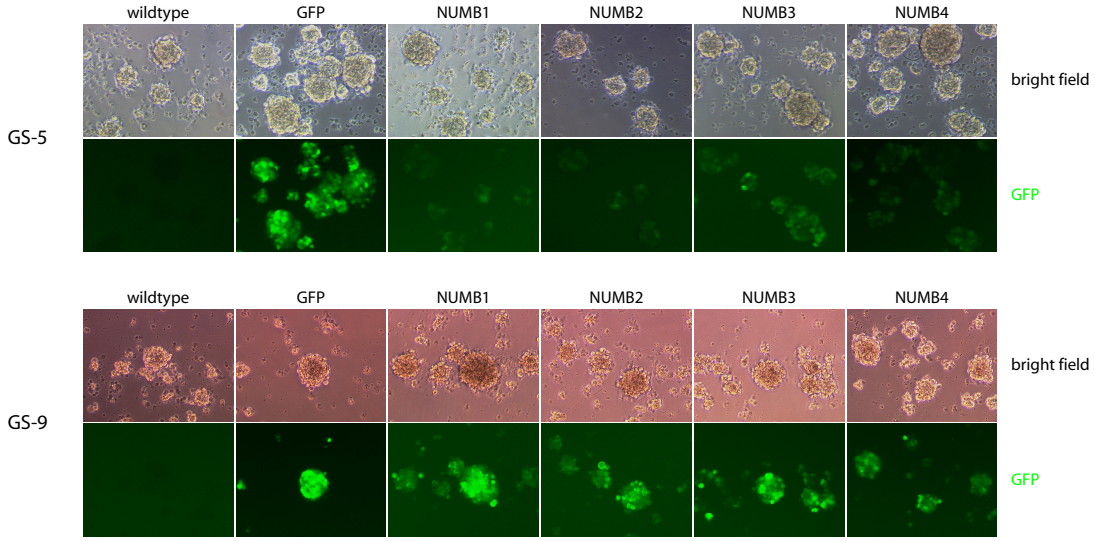

Figure 3.20.: **NUMB overexpression in gliomaspheres.** Cell lines GS-5 and GS-9 were lentivirally transduced with NUMB-GFP or GFP alone at a MOI of 5. Images were taken 48 hours after infection.

4. Discussion

The aim of this study was to specifically block multiple pathways involved in the maintenance of glioma stem cells by overexpression of NUMB in a gene therapy-like experiment design.

First, expression of NUMB in patient samples was briefly characterized. NUMB2 and NUMB4 were then successfully overexpressed in human U87 glioma cells. This alteration did not impair proliferation *in vitro* or *in vivo* nor could it induce differentiation towards a glial or neural phenotype. Hedgehog, Notch and p53 signalling were not altered by overexpression of NUMB in U87 glioma cells, but downregulation of Notch signalling was observed in human U251 and U373 glioma cells.

As a possibly more suitable model, gliomaspheres grown in NSC medium were used. Analysis of public microarray data suggested that these cells express NUMB at lower levels and show higher activation of NUMB-related pathways. After overexpression of NUMB isoforms in gliomaspheres, however, no change in phenotype could be observed.

4.1. NUMB expression in patient samples and cell lines

Little is known about NUMB in the context of gliomas. Only one study briefly examined NUMB expression in paraffin section of astrocytic tumors and found NUMB to be expressed in GBM samples [91].

In this thesis, NUMB expression was determined in biopsy material on the mRNA and protein levels. It was found that NUMB is expressed in GBM and at levels comparable to those of normal brain. Western blotting experiments showed that of all four human NUMB isoforms NUMB2 and NUMB4 are predominantly expressed. This finding is surprising because NUMB2/4 levels have previously been shown to be typical for differentiated cells while they are not expressed in murine neural progenitor cells [87]. In GBM, one would expect molecular signatures of undifferentiated cells.

However, it might be possible that loss of NUMB expression is masked by normal brain cells with high levels of NUMB2/4. Similarily, if downregulation of NUMB is a feature of a stem-like phenotype, then one would expect only cancer stem cells to lack NUMB expression.

Since CSCs are considered to be only a minor fraction of the tumor [16], the remaining tumor cells would mask the loss of NUMB in CSCs.

Because of this, we decided to compare NUMB expression in different glioma cell lines which either show a stem-like phenotype or do not. When comparing microarray data from a published study [47], NUMB levels were found to be lower in gliomaspheres grown in medium designed for culturing neural stem cells than in glioma cell lines in serum-containing medium. Hierarchical clustering reliably distinguished both types of cell lines only based on different NUMB probes.
Additionally, different stem cell markers and Notch signalling genes were expressed at higher levels in gliomaspheres, underscoring their stem-like gene expression pattern. At the protein level, our own experiments showed that gliomaspheres do indeed express less NUMB than does the common U87 glioma cell line. However, also here NUMB2/4 isoforms were predominant and no switch from 'adult' NUMB2/4 to 'embryonal' NUMB1/3 could be seen.

In conclusion, it seems that NUMB is ubiquitously expressed in normal and malignant brain tissue and different in vitro glioma models. However, NUMB might be downregulated in cells with a stem-like phenotype compared to serum-cultured cells.
These findings are consistent with expression data from paraffin sections of gliomas [91], but contrary to studies in other tumor types. In breast cancer, loss of NUMB expression was observed in nearly 40% of the examined samples [62] and in salivary gland carcinomas, only moderate NUMB staining (compared to normal glands) was found in the majority of cases [52]. It is thus possible that extensive loss of NUMB is a feature of cancers of epithelial origin.

As far as NUMB levels in CSCs are concerned, our results are similar to the observation made in myeloid leukemia, in which reduced NUMB levels correlated with a stem-like phenotype [93].

4.2. Overexpression of NUMB in adherent glioma cell lines

Based upon published interactions of NUMB with glioma related pathways and because of its role during asymmetric cell division during neurogenesis, it was hypothesized that NUMB overexpression in glioma models could favor a more differentiated phenotype or direct cells towards growth arrest or apoptosis.

To test this, NUMB was first introduced into adherent glioma cell lines by lentiviral infection with a GFP-fusion protein. This overexpression did not stop cells from proliferating. Transduced human U87 glioma cells showed unchanged growth rates compared to wildtype cells and GFP controls. On the single cell level, Ki-67 expression in transduced U251 cells

indicated continued cell cycle progression and the fraction of M phase cells in NUMB overexpressing U87 cells stained for phospho-Histone H3 was similar to wild-type cells. Furthermore, no signs of differentiation were observed in NUMB transduced U87 cell lines. Morphologic changes could not be assessed. The glial marker GFAP and neuron-specific β-Tubulin III were not upregulated by NUMB overexpression.

Tumorigenicity of NUMB overexpressing cells was tested in an intracranial xenograft model. U87-NUMB cells were stereotactically implanted into nude rats. Tumor take was 100% for transduced cells and controls. Survival time until the onset of clinical symptoms was for similar for wildtype and NUMB2 overexpressing tumors and even shorter in U87-NUMB4 cells. The morphology of the tumors as seen on MRI remained unchanged. Merely histomorphological differences were found between GFP controls and NUMB4 tumors. Cell density was much lower in these tumors with enclosed pseudocystic areas. Accordingly, NUMB overexpression did change the histological appearance of U87 xenografts, but no therapeutically relevant effect was seen.

In comparison, two studies used NUMB overexpression in other cancers and could partly show effects on proliferation. Pece and colleagues introduced NUMB1 into primary breast cancer cells and found impaired clonogenicity, but only when NUMB expression was low in the parental cells [62]. Since NUMB levels are high in the U87 cell line we used, this might explain failure to respond to NUMB overexpression.

Marcotullio and colleagues overexpressed NUMB2 in a medulloblastoma cell line and observed impaired clonogenicity, decreased BrdU uptake and increase of β-tubulin III expression [53]. This means that NUMB2 was capable of slowing down proliferation and inducing differentiation in a medulloblastoma model. In gliomas, we could not recapitulate these findings. It should be noted, however, that the underlying tumor biology and the putative cell of origin differ significantly between the cancers discussed and compared above.

4.3. Pathway interactions in experimental gliomas

We further aimed to investigate if published interactions of NUMB with relevant signalling pathways could also be found in gliomas.

Notch signalling Levels of HES1 and HES5 transcription factors, which are effectors of NOTCH signalling, were found to be downregulated by NUMB4, even though no statistical significance was reached because the experiment was not repeated. These results are consistent with published data [56, 55, 61]. However, HES levels in U87 wildtype cells were undetectable, thus no regulation could be demonstrated. This is most likely due to

limited sensitivity of the PCR reaction because inhibition of the pathway by knockdown of NOTCH1 is sufficient to decelerate growth of U87 cells [66]. However, the same study showed that U87 cells had the lowest activity of NOTCH signalling among different glioma cell lines.

Hedgehog signalling Hedgehog signalling activity was examined by a reporter gene assay in U87 cells. A GLI-responsive luciferase construct was used to detect changes in the expression of GLI1 and GLI2 transcription factors, which are effectors of the pathway. Additionally, sonic hedgehog (SHH) was used for stimulation of the pathway because it had been shown previously that Hedgehog ligands are not expressed in vitro [9].

To exclude methodological errors, we included two positive controls in our experiments. Induction of the reporter gene could be demonstrated by co-transfection of GLI1, proving that the construct works properly with the setup we used. Then it was tested if SHH co-transfection would stimulate the pathway and subsequently induce the luciferase construct. This experiment was performed in 293T cells, in which an approximately 5-fold induction was previously demonstrated [53]. In our experiments, a reproducible 1.4-fold induction was observed. The limited dynamics are maybe due to the use of full length SHH mRNA co-transfection which is possibly less potent than the N-terminal cDNA fragments or recombinant SHH used by Marcotullio and colleagues.

In the actual experiment, we observed a slight but not significant upregulation of the reporter in U87 cells by SHH stimulation. Induction of the same Gli-responsive reporter in U87 cells by recombinant SHH was less than 2-fold in one study and thus comparable to our results [9].

Additional co-transfection of NUMB isoforms did not significantly alter luciferase activity. This is in contrast to the literature because NUMB is supposed to antagonize Hedgehog signalling by ubiquitylation of GLI1 [53]. In their study, the authors observed downregulation of GLI levels by NUMB in 293T cells and a growth-inhibitory effect in medulloblastoma cell lines. Neither effect could be recapitulated in the U87 glioma cell line by our experiments.

It is of course possible that this mechanism is specific to a certain cellular context which is not given in U87 cells. The question is whether Hedgehog signalling itself is not active in U87 or if NUMB does not interfere with it. In general, some studies argue that Hedgehog signalling plays a minor role in GBM as compared to less malignant astrocytic tumors [26, 42], while others found a positive correlation between malignancy and Hedgehog activity [20, 90]. Furthermore, there is evidence from two studies who claim that growth of U87 cells can be inhibited by chemical blockade of the pathway [22, 8]. Thus, it is likely that Hedgehog signalling is active in this cell line, but NUMB overexpression is not an appropriate way to

interfere with it. However, interaction of NUMB and Hedgehog signalling seems not to be restricted to medulloblastoma since an inverse correlation of NUMB levels and CSC numbers was also described in myeloid leukemia [93].

Taken together, both Notch and Hedgehog signalling are likely to be active in U87 at a basal level, but overexpression of NUMB did not yield detectable effects with respect to proliferation. Mechanistically, NUMB did not influence Hedgehog signalling in U87 while changes in Notch transcription factors could not be detected. A possible reason for failure to efficiently block Hedgehog (and Notch) signalling could be the lack of the E3 ligase ITCH, which is necessary for NUMB-mediated degradation of both NOTCH1 and GLI1 [56, 53].

p53 A recent publication has reported that NUMB is capable of stabilizing the tumor suppressor p53 by entering a tricomplex with MDM2 [21]. This requires, of course, unhampered p53 function, which is altered frequently by mutations in gliomas.

Therefore, we examined p53 protein levels in response to overexpression of NUMB2 or NUMB4 in U87 cells which is known to have wildtype p53 on both alleles [57]. No alterations were detected based on expression levels. However, the cells were not put under stress (e.g. by addition of chemotherapeutic drugs) to assess a differential p53 response nor did we perform functional assays of p53 activity. It should also be noted that Colaluca and colleagues could only find an increase in p53 expression in breast cancer cells that displayed no or only weak expression of NUMB [21]. Again, this is not the case in U87 cells and might explain missing upregulation of p53.

4.4. Model considerations

No striking effects were seen in U87 cells with respect to clinically relevant readouts such as proliferation or tumorigenicity. Likewise, no relevant functional interactions could be observed. Before concluding from these experiments, some characteristics of adherent glioma cell lines in general and use of U87 in particular must be considered.

First, there is a significant baseline level of NUMB expression in U87 cells. Even though not all four human NUMB isoforms can be distinguished by protein size on western blots, it was observed that mainly those isoforms that reportedly induce differentiation in neural progrenitor cells during mouse embryonal development (i.e. NUMB2 and NUMB4) [87] are expressed. This was confirmed by comparing mRNA levels using isoform specific realtime PCR. It indicates that U87 cells are well adapted to high levels of NUMB2/4 and there might be a ceiling effect that cannot be overcome even by strong overexpression of NUMB.

Second, U87 cells grown under the conditions we used (i.e. as monolayers in medium containing fetal bovine serum) have not been shown to exhibit stem cell properties. While self renewal is obviously a feature of these cells, one can not be sure whether U87 cells actually are in an undifferentiated state and possess the ability to differentiate into neurons or glial cells.

On the other hand, some authors argue that cancer-stem like cells can be derived ex vivo from U87 xenografts [1] or directly in vitro [12]. However, these cells have been selected by CD133 expression, whose function as a glioma stem cell markers is controversely discussed. The differentiation potential of putative U87 derived cancer stem cells was not tested (Manuel Guzmán, personal communication).

Therefore, adherent glioma cell lines are not well suited for experiments in the context of the cancer stem cell hypothesis. Other models, namely glioma cells cultured in NSC medium provide a better starting point.

4.5. NUMB overexpression in gliomaspheres

Because of these drawbacks, NUMB was overexpressed in different gliomaspheres. No alteration of the morphology was seen. According to the hypothesis, failure of the cells infected as single cell suspension to form spheroids or adhesion to the bottom of the flask due to induction of differentiation was expected.
Neither one was observed and even though no characterization of proliferation or gene expression was performed, some conclusions can be drawn from the experiments.

Nonadherent sphere-like growth is generally associated with stem cell properties of the cells making up the spheroid. Even though no clear mechanistic links are published, most studies show that cells losing stem cell properties and undergoing differentiation will eventually settle down and adhere to the surface of the culture dish. Laks and colleagues reported that the ability of primary glioma cells from surgical specimens to form neurospheres in vitro is correlated to clinical outcome [46].

Only one other study has addressed the role of NUMB in CSCs. Zhao and colleagues overexpressed NUMB in a model of chronic myeloid leukemia which resulted in decreased colony numbers in a clonogenicity assay [93]. We have not performed a formal clonogenicity assay, but it seemed as if dissociated NUMB transduced gliomaspheres reformed spheroids from this single cell suspension.

In conclusion, NUMB transduced neurospheres maintained their phenotype. Therefore, NUMB overexpression does not seem to alter gliomasphere behavior in a therapeutically relevant manner.

4.6. Conclusions

NUMB overexpression could not influence the phenotype of gliomaspheres or adherent glioma cell lines in any way that would be of clinical interest. Several aspects can be discussed as possible reasons for this failure.

First, the role of NUMB during mammalian neurogenesis is controversial. While it has been shown that NUMB determines cell fate in hematopoetic and muscle cells, asymmetric localization of NUMB in the mammalian brain has been observed but is maybe not linked to cell fate specification (reviewed in [45]). Its suggested function would then be maintenance of epithelial polarity by coordination of cadherins.

Second, even if NUMB orchestrates cell fate during asymmetric cell division, it does not necessarily trigger differentiation. Another stimulus for the cell to decide on a asymmetric division might well be necessary. This could be, for example, factors known to excert these effects physiologically such as retinoic acid, BDNF or NGF.

Third, some literature shows that NUMB requires phosphorylation in order to be asymmetrically distributed around the cell membrane [80]. Using NUMB mutants with defect phosphorylation sites impaired asymmetric segregation. In our study, phosphorylation was not monitored and wildtype NUMB isoforms were used. It might be possible that cells were still able to generate progeny receiving no NUMB during mitosis and thus maintained a stem-like phenotype. This would implicate that the effects of NUMB are dependent on the cell cycle context. This is likely given the fact that Drosophila sensory organ progenitor (SOP) cells undergo two consecutive cell divisions in each of which NUMB levels determine their fate differently.

These issues challenge the main hypothesis of this thesis, claiming that overexpression of NUMB will induce differentiation in tumor cells. Too little is currently known about the role of NUMB with respect to regulation and maintenance of stem cells, let aside their malignant counterparts in gliomas. Further research in the field of developmental neuroscience, stem cell biology and cancer research will hopefully further elucidate some of the mechanisms involved. The results of this study, however, suggest that NUMB is not a promising therapeutic target in GBM.

5. Summary

Introduction Glioblastoma multiforme is the most frequent primary CNS tumor in adults characterized by highly invasive growth with dismal prognosis. Despite multimodal treatment with surgery, radiation and chemotherapy median survival is about 15 months.

The recently developed cancer stem cell hypothesis postulates a new perspective towards the pathogenesis of this aggressive tumor. It claims that only a small subpopulation of tumor cells is capable of propagating the disease. These cells were observed to have stem-cell properties (namely capacity of self-renewal and multilineage differentiation). One of the mechanisms for self-renewal is asymmetric cell division. Additionally, developmental signalling pathways (such as Notch or Hedgehog) regulate stem-cell maintenance physiologically and are reportedly active in gliomas.

Aims Because of these similarities, the goal of this thesis was to study the cell fate determinant NUMB, which is involved in asymmetric cell division and interacts with Notch and Hedgehog signalling, for therapeutic suitability. By ectopic expression of NUMB isoforms in experimental tumors using lentiviral gene transfer, effects of NUMB on proliferation, differentiation and activity of the before mentioned signalling pathways were to be characterized.

Methods Expression of NUMB and its isoforms was studied in patient biopsies and different glioma models by realtime PCR, western blotting and immunofluorescence. Additionally, public microarray data of gliomaspheres and serum-cultured glioma cell lines were analyzed.

Then, adherent glioma cell lines were virally transduced by different NUMB isoforms. Proliferation was documented by growth curves and immunohistochemistry. Cell lines were orthotopically implanted into the brains of immunoincompetent rats in order to assess tumorigenicity. MR imaging and histology were used to study tumor morphology. Finally, NUMB was overexpressed in gliomaspheres with known stem cell properties to assess phenotypic changes.

Results NUMB is expressed in patient material, adherent glioma cell lines as well as in gliomaspheres. NUMB2 and NUMB4 isoforms dominated in all samples. In microarray

gene expression data of gliomaspheres, slightly lower levels of NUMB were observed, which correlated inversely with stem cell markers and Notch-related genes.

After overexpression of NUMB2 or NUMB4 in U87 glioma cells, no significant change of growth kinetics of differentiation could be observed. Morphologically and with respect to glial and neural differentiation markers, no differences were seen. NUMB2- and NUMB4-overexpressing U87 cells were tumorigenic after intracranial implantation into nude rats. Here, histomorphological differences were observed by terms of a loose, possibly pseudocystic, cellular matrix in transduced tumors. With regard to survival, no significant effects of NUMB overexpression were seen, but animals bearing NUMB4 tumors developed symptoms earlier.

However, existence of cancer stem cells in the U87 cells used is uncertain due to growth in serum containing medium. Hence, all four human NUMB isoforms were also overexpressed in gliomaspheres grown in neural stem cell medium. No morphologic changed could be shown which would have indicated differentation or impaired self-renewal.

Functionally, Notch and Hedgehog activity and p53 protein level were studied in adherent glioma cells after NUMB overexpression. In U251 and U373 cell lines, reduced transcription of HES1, a Notch effector transcription factor, was seen. Experiments using a reporter gene for Hedgehog activity in U87 cells did not suggest inhibition of the pathway by NUMB. Similarily, p53 expression was unchanged.

Conclusion NUMB seems to be regularly expressed in gliomas. Even though we detected reduced levels in stem-like glioma cells, no loss of NUMB expression was seen similar to published observations in epithelial cancers.

Overexpression of NUMB in different glioma models did not show any effects with respect to the hypotheses. Tumorigenicity of transduced cells was not impaired and differentiation, even of stem cell-rich cell cultures, did not occur. With regard to published interactions with glioma-relevant signalling pathways, merely inhibition of Notch signalling could be shown, other predescribed interactions could not be recapitulated in glioma cell lines.

In this thesis, the role of NUMB as a putative tumor suppressor was studied in the context of experimental gliomas in vitro and in vivo. Based upon the results from our experiments, however, NUMB does not appear to be suited as a therapeutic target in malignant gliomas.

6. Zusammenfassung

Einführung Glioblastoma multiforme ist der häufigste primäre Hirntumor bei Erwachsenen und gekennzeichnet durch eine infauste Prognose bei extrem infiltrativem Wachstum. Trotz multimodaler Therapie mit Resektion, Bestrahlung und Chemotherapie liegt das mediane Überleben bei weniger als zwei Jahren.

Die in den letzten Jahren formulierte Krebsstammzellhypothese hat der Gliomforschung eine neue Sichtweise auf die Pathologie dieses aggressiven Tumors gegeben. Sie sagt aus, dass nur eine kleine Subpopulation aller Tumorzellen in der Lage ist, diesen zu propagieren. Bei diesen Zellen werden Stammzelleigenschaften (d.h. die Fähigkeit zur Selbsterneuerung und zur Differenzierung in multiple Zelltypen) beobachtet. Einer der Mechanismen zur Selbsterneuerung ist asymmetrische Zellteilung. Außerdem sind embryonale Signalkaskaden (z.B. Notch oder Hedgehog) in normalen Stammzellen und in Gliomzellen aktiv.

Zielsetzung Aufgrund dieser Ähnlichkeiten war das Ziel der vorliegenden Arbeit, die Zellschicksaldeterminante NUMB, welche asymmetrische Zellteilung kontrolliert und mit den Notch und Hedgehog Signalwegen interagiert, auf ihre Eignung als therapeutisches Gen zu untersuchen. Durch ektope Expression von verschiedenen NUMB Isoformen in experimentellen Tumoren mittels lentiviralen Gentransfer sollten die Auswirkungen von NUMB auf Proliferation, Differenzierung und Aktivität der erwähnten Signalwege charakterisiert werden.

Methodik Die Expression von NUMB und seinen Isoformen wurde in Patientenmaterial sowie verschiedenen in vitro Gliommodellen mittels realtime-PCR, Western Blot und Immunfluoreszenz untersucht. Zusätzlich wurden öffentliche Microarray-Daten von Gliomspheroiden und Serumkulturen analysiert.

Dann wurden adhärente Gliomzellen viral mit verschiedenen NUMB Isoformen transduziert. Zellproliferation wurde in Wachstumskurven und immunocytochemisch dokumentiert. Anschließend wurden die Zelllinien orthotop in immunoinkompetente Ratten implantiert, um ihre Tumorigenität zu bestimmen. Kernspintomographische Morphologie und Histologie der Tumoren wurden erfasst. Schließlich wurde NUMB

in Gliomspheroiden mit dokumentierten Stammzelleigenschaften überexprimiert, um morphologische Veränderungen zu erfassen.

Ergebnisse NUMB wird in Biopsiematerial, adhärenten Gliomzelllinien und Gliomspheroiden exprimiert. NUMB2 und NUMB4 Isoformen dominieren in allen untersuchten Proben. In Gliomspheroiden wurden leicht niedrige NUMB Level gemessen, welche invers mit Stammzellmarkern und Notch-relevanten Genen korrelierten.

Nach Überexpression von NUMB2 und NUMB4 in U87 Gliomzellen konnte keine signifikante Veränderung von Wachstumsparametern und Differenzierungsgrad gezeigt werden. Morphologisch und in der Expression von glialen oder neuronalen Differenzierungsmarkern wurden keine Unterschiede beobachtet. NUMB2- und NUMB4-überexprimierende U87 Zellen waren tumorigen nach intrakranieller Implantation in Nacktratten. Hier konnten histomorphologische Unterschiede mit aufgelockerter Binnenstruktur, am ehesten im Sinne von Pseudozysten, in NUMB4-Tumoren beobachtet werden. Im Hinblick auf die Überlebenszeit bis zum Eintritt klinischer Symptome konnten keine signifikanten Unterschiede festgestellt werden, wenn auch Tiere mit NUMB4-Tumoren durchschnittlich früher Symptome entwickelten.

Die Persistenz von Krebsstammzellen in den verwendeten U87 Zellen ist allerdings aufgrund ihrer Kultur in serumhaltigem Medium ungewiss. Deshalb wurden alle vier humanen NUMB Isoformen auch in Gliomspheroiden überexprimiert. Diese zeigten daraufhin keine morphologischen Veränderungen, die auf eine Ausdifferenzierung hätten hinweisen können.

Funktional wurden die Aktivität des Notch- und Hedgehog-Signalweges sowie Proteinlevel des Tumorsuppressors p53 in adhärenten Gliomzellen nach NUMB-Überexpression untersucht. In U251 und U373 Zelllinien konnte eine Reduktion des Transkriptionsfaktors HES1 beobachtet werden, einem Effektor des Notch Signalweges. Experimente mit einem Reportergen für den Hedgehog-Signalweg in U87 Zellen konnten keine Inhibition durch NUMB erkennen lassen. Ebenso war die Expression von p53 unverändert.

Diskussion NUMB scheint regelhaft in Glioblastomen exprimiert zu werden. Wenn auch erniedrigte Level in stammzellartigen Krebszellen auftreten, konnten wir keinen Verlust von NUMB ähnlich den publizierten Ergebnissen in einigen epithelialen Neoplasien nachweisen.

Überexpression von NUMB in verschiedenen Gliommodellen zeigte keine Effekte im Sinne der Hypothesen. Die Tumorigenität der infizierten Zellen blieb erhalten und Differenzierung, auch krebsstammzellreicher Zellkulturen, blieb aus. Im Hinblick auf die veröffentlichten Interaktionen mit Gliom-relevanten Signalwegen konnte lediglich die

Inhibition des Notch-Signalweges gezeigt werden, andere beschriebene Wechselwirkungen konnten in Gliomzellen nicht rekapituliert werden.

In dieser Arbeit wurde zum ersten Mal gezielt die Rolle des putativen Tumorsuppressors NUMB in Glioblastomen deskriptiv und interventionell in vitro und in vivo untersucht. Eine Eignung als therapeutisches Gen im Kontext hochmaligner Gliome scheint jedoch auf Basis der Ergebnisse unwahrscheinlich.

7. References

[1] Tania Aguado, Arkaitz Carracedo, Boris Julien, Guillermo Velasco, Garry Milman, Raphael Mechoulam, Luis Alvarez, Manuel Guzmán, and Ismael Galve-Roperh. Cannabinoids induce glioma stem-like cell differentiation and inhibit gliomagenesis. *J Biol Chem*, 282(9):6854–6862, Mar 2007.

[2] Adan Aguirre, Maria E Rubio, and Vittorio Gallo. Notch and egfr pathway interaction regulates neural stem cell number and self-renewal. *Nature*, 467(7313):323–327, Sep 2010.

[3] S. Artavanis-Tsakonas, M. D. Rand, and R. J. Lake. Notch signaling: cell fate control and signal integration in development. *Science*, 284(5415):770–776, Apr 1999.

[4] Robert M Bachoo, Elizabeth A Maher, Keith L Ligon, Norman E Sharpless, Suzanne S Chan, Mingjian James You, Yi Tang, Jessica DeFrances, Elizabeth Stover, Ralph Weissleder, David H Rowitch, David N Louis, and Ronald A DePinho. Epidermal growth factor receptor and ink4a/arf: convergent mechanisms governing terminal differentiation and transformation along the neural stem cell to astrocyte axis. *Cancer Cell*, 1(3):269–277, Apr 2002.

[5] Katrin M Baltz, Matthias Krusch, Anita Bringmann, Peter Brossart, Frank Mayer, Mercedes Kloss, Tina Baessler, Ingrid Kumbier, Andrea Peterfi, Susan Kupka, Stefan Kroeber, Dagmar Menzel, Markus P Radsak, Hans-Georg Rammensee, and Helmut R Salih. Cancer immunoediting by gitr (glucocorticoid-induced tnf-related protein) ligand in humans: Nk cell/tumor cell interactions. *FASEB J*, 21(10):2442–2454, Aug 2007.

[6] Mahmud Bani-Yaghoub, Chris J Kubu, Rebecca Cowling, Jennifer Rochira, George N Nikopoulos, Stephen Bellum, and Joseph M Verdi. A switch in numb isoforms is a critical step in cortical development. *Dev Dyn*, 236(3):696–705, Mar 2007.

[7] Shideng Bao, Qiulian Wu, Roger E McLendon, Yueling Hao, Qing Shi, Anita B Hjelmeland, Mark W Dewhirst, Darell D Bigner, and Jeremy N Rich. Glioma stem cells promote radioresistance by preferential activation of the dna damage response. *Nature*, 444(7120):756–760, Dec 2006.

[8] Eli E Bar, Aneeka Chaudhry, Alex Lin, Xing Fan, Karisa Schreck, William Matsui, Angelo L Vescovi, Sara Piccirillo, Francesco Dimeco, Alessandro Olivi, and Charles G Eberhart. Cyclopamine-mediated hedgehog pathway inhibition depletes stem-like cancer cells in glioblastoma. *Stem Cells*, Jul 2007.

[9] Oren J Becher, Dolores Hambardzumyan, Elena I Fomchenko, Hiroyuki Momota, Lori Mainwaring, Anne-Marie Bleau, Amanda M Katz, Mark Edgar, Anna M Kenney, Carlos

Cordon-Cardo, Ron G Blasberg, and Eric C Holland. Gli activity correlates with tumor grade in platelet-derived growth factor-induced gliomas. *Cancer Res*, 68(7):2241–2249, Apr 2008.

[10] Dagmar Beier, Peter Hau, Martin Proescholdt, Annette Lohmeier, Jörg Wischhusen, Peter J Oefner, Ludwig Aigner, Alexander Brawanski, Ulrich Bogdahn, and Christoph P Beier. Cd133(+) and cd133(-) glioblastoma-derived cancer stem cells show differential growth characteristics and molecular profiles. *Cancer Res*, 67(9):4010–4015, May 2007.

[11] P. Benda, J. Lightbody, G. Sato, L. Levine, and W. Sweet. Differentiated rat glial cell strain in tissue culture. *Science*, 161(839):370–371, Jul 1968.

[12] Julian Bertrand, Gaëlle Begaud-Grimaud, Barbara Bessette, Mireille Verdier, Serge Battu, and Marie-Odile Jauberteau. Cancer stem cells from human glioma cell line are resistant to fas-induced apoptosis. *Int J Oncol*, 34(3):717–727, Mar 2009.

[13] Winfried R Beyer, Manfred Westphal, Wolfram Ostertag, and Dorothee von Laer. Oncoretrovirus and lentivirus vectors pseudotyped with lymphocytic choriomeningitis virus glycoprotein: generation, concentration, and broad host range. *J Virol*, 76(3):1488–1495, Feb 2002.

[14] R. Bjerkvig, A. Tønnesen, O. D. Laerum, and E. O. Backlund. Multicellular tumor spheroids from human gliomas maintained in organ culture. *J Neurosurg*, 72(3):463–475, Mar 1990.

[15] D. Bonnet and J. E. Dick. Human acute myeloid leukemia is organized as a hierarchy that originates from a primitive hematopoietic cell. *Nat Med*, 3(7):730–737, Jul 1997.

[16] Christopher Calabrese, Helen Poppleton, Mehmet Kocak, Twala L Hogg, Christine Fuller, Blair Hamner, Eun Young Oh, M. Waleed Gaber, David Finklestein, Meredith Allen, Adrian Frank, Ildar T Bayazitov, Stanislav S Zakharenko, Amar Gajjar, Andrew Davidoff, and Richard J Gilbertson. A perivascular niche for brain tumor stem cells. *Cancer Cell*, 11(1):69–82, Jan 2007.

[17] Kate A Carey, Michelle M Farnfield, Sarah D Tarquinio, and David Cameron-Smith. Impaired expression of notch signaling genes in aged human skeletal muscle. *J Gerontol A Biol Sci Med Sci*, 62(1):9–17, Jan 2007.

[18] Michel Cayouette and Martin Raff. Asymmetric segregation of numb: a mechanism for neural specification from drosophila to mammals. *Nat Neurosci*, 5(12):1265–1269, Dec 2002.

[19] Juxiang Chen, Jian Xu, Wei Zhao, Guohan Hu, Haipeng Cheng, Ying Kang, Yi Xie, and Yicheng Lu. Characterization of human lnx, a novel ligand of numb protein x that is downregulated in human gliomas. *Int J Biochem Cell Biol*, 37(11):2273–2283, Nov 2005.

[20] Virginie Clement, Pilar Sanchez, Nicolas de Tribolet, Ivan Radovanovic, and Ariel Ruiz i Altaba. Hedgehog-gli1 signaling regulates human glioma growth, cancer stem cell self-renewal, and tumorigenicity. *Curr Biol*, 17(2):165–172, Jan 2007.

[21] Ivan N Colaluca, Daniela Tosoni, Paolo Nuciforo, Francesca Senic-Matuglia, Viviana Galimberti, Giuseppe Viale, Salvatore Pece, and Pier Paolo Di Fiore. Numb controls p53 tumour suppressor activity. *Nature*, 451(7174):76–80, Jan 2008.

[22] N. Dahmane, P. Sánchez, Y. Gitton, V. Palma, T. Sun, M. Beyna, H. Weiner, and A. Ruiz i Altaba. The sonic hedgehog-gli pathway regulates dorsal brain growth and tumorigenesis. *Development*, 128(24):5201–5212, Dec 2001.

[23] C. Dai, J. C. Celestino, Y. Okada, D. N. Louis, G. N. Fuller, and E. C. Holland. Pdgf autocrine stimulation dedifferentiates cultured astrocytes and induces oligodendrogliomas and oligoastrocytomas from neural progenitors and astrocytes in vivo. *Genes Dev*, 15(15):1913–1925, Aug 2001.

[24] M. J L de Hoon, S. Imoto, J. Nolan, and S. Miyano. Open source clustering software. *Bioinformatics*, 20(9):1453–1454, Jun 2004.

[25] S. E. Dho, M. B. French, S. A. Woods, and C. J. McGlade. Characterization of four mammalian numb protein isoforms. identification of cytoplasmic and membrane-associated variants of the phosphotyrosine binding domain. *J Biol Chem*, 274(46):33097–33104, Nov 1999.

[26] M. Ehtesham, A. Sarangi, J. G. Valadez, S. Chanthaphaychith, M. W. Becher, T. W. Abel, R. C. Thompson, and M. K. Cooper. Ligand-dependent activation of the hedgehog pathway in glioma progenitor cells. *Oncogene*, 26(39):5752–5761, Aug 2007.

[27] Xing Fan, William Matsui, Leila Khaki, Duncan Stearns, Jiong Chun, Yue-Ming Li, and Charles G Eberhart. Notch pathway inhibition depletes stem-like cells and blocks engraftment in embryonal brain tumors. *Cancer Res*, 66(15):7445–7452, Aug 2006.

[28] Xing Fan, Irina Mikolaenko, Ihab Elhassan, Xingzhi Ni, Yunyue Wang, Douglas Ball, Daniel J Brat, Arie Perry, and Charles G Eberhart. Notch1 and notch2 have opposite effects on embryonal brain tumor growth. *Cancer Res*, 64(21):7787–7793, Nov 2004.

[29] P. Good, A. Yoda, S. Sakakibara, A. Yamamoto, T. Imai, H. Sawa, T. Ikeuchi, S. Tsuji, H. Satoh, and H. Okano. The human musashi homolog 1 (msi1) gene encoding the homologue of musashi/nrp-1, a neural rna-binding protein putatively expressed in cns stem cells and neural progenitor cells. *Genomics*, 52(3):382–384, Sep 1998.

[30] Corinne E Griguer, Claudia R Oliva, Eric Gobin, Pascale Marcorelles, Dale J Benos, Jack R Lancaster, and G. Yancey Gillespie. Cd133 is a marker of bioenergetic stress in human glioma. *PLoS One*, 3(11):e3655, 2008.

[31] H. S. Günther, N. O. Schmidt, H. S. Phillips, D. Kemming, S. Kharbanda, R. Soriano, Z. Modrusan, H. Meissner, M. Westphal, and K. Lamszus. Glioblastoma-derived stem cell-enriched cultures form distinct subgroups according to molecular and phenotypic criteria. *Oncogene*, Nov 2007.

[32] Jurre Hageman, Bart J Eggen, Tom Rozema, Kevin Damman, Harm H Kampinga, and Robert P Coppes. Radiation and transforming growth factor-beta cooperate in transcriptional activation of the profibrotic plasminogen activator inhibitor-1 gene. *Clin Cancer Res*, 11(16):5956–5964, Aug 2005.

[33] Monika E Hegi, Annie-Claire Diserens, Thierry Gorlia, Marie-France Hamou, Nicolas de Tribolet, Michael Weller, Johan M Kros, Johannes A Hainfellner, Warren Mason, Luigi Mariani, Jacoline E C Bromberg, Peter Hau, René O Mirimanoff, J. Gregory Cairncross, Robert C Janzer, and Roger Stupp. Mgmt gene silencing and benefit from temozolomide in glioblastoma. *N Engl J Med*, 352(10):997–1003, Mar 2005.

[34] Houman D Hemmati, Ichiro Nakano, Jorge A Lazareff, Michael Masterman-Smith, Daniel H Geschwind, Marianne Bronner-Fraser, and Harley I Kornblum. Cancerous stem cells can arise from pediatric brain tumors. *Proc Natl Acad Sci U S A*, 100(25):15178–15183, Dec 2003.

[35] C. Hirschmann-Jax, A. E. Foster, G. G. Wulf, J. G. Nuchtern, T. W. Jax, U. Gobel, M. A. Goodell, and M. K. Brenner. A distinct "side population" of cells with high drug efflux capacity in human tumor cells. *Proc Natl Acad Sci U S A*, 101(39):14228–14233, Sep 2004.

[36] E. C. Holland, J. Celestino, C. Dai, L. Schaefer, R. E. Sawaya, and G. N. Fuller. Combined activation of ras and akt in neural progenitors induces glioblastoma formation in mice. *Nat Genet*, 25(1):55–57, May 2000.

[37] T. Imai, A. Tokunaga, T. Yoshida, M. Hashimoto, K. Mikoshiba, G. Weinmaster, M. Nakafuku, and H. Okano. The neural rna-binding protein musashi1 translationally regulates mammalian numb gene expression by interacting with its mrna. *Mol Cell Biol*, 21(12):3888–3900, Jun 2001.

[38] Jane E Johnson. Numb and numblike control cell number during vertebrate neurogenesis. *Trends Neurosci*, 26(8):395–396, Aug 2003.

[39] T. Juven-Gershon, O. Shifman, T. Unger, A. Elkeles, Y. Haupt, and M. Oren. The mdm2 oncoprotein interacts with the cell fate regulator numb. *Mol Cell Biol*, 18(7):3974–3982, Jul 1998.

[40] Masayuki Kanamori, Tomohiro Kawaguchi, Janice M Nigro, Burt G Feuerstein, Mitchel S Berger, Lucio Miele, and Russell O Pieper. Contribution of notch signaling activation to human glioblastoma multiforme. *J Neurosurg*, 106(3):417–427, Mar 2007.

[41] Camilla Karlsson, Camilla Brantsing, Teresia Svensson, Helena Brisby, Julia Asp, Tommi Tallheden, and Anders Lindahl. Differentiation of human mesenchymal stem cells and articular chondrocytes: analysis of chondrogenic potential and expression pattern of differentiation-related transcription factors. *J Orthop Res*, 25(2):152–163, Feb 2007.

[42] Masateru Katayama, Kazunari Yoshida, Hisatsugu Ishimori, Makoto Katayama, Takeshi Kawase, Jun Motoyama, and Hiroyuki Kamiguchi. Patched and smoothened mrna expression in human astrocytic tumors inversely correlates with histological malignancy. *J Neurooncol*, 59(2):107–115, Sep 2002.

[43] K. W. Kinzler, J. M. Ruppert, S. H. Bigner, and B. Vogelstein. The gli gene is a member of the kruppel family of zinc finger proteins. *Nature*, 332(6162):371–374, Mar 1988.

[44] P. Kleihues and H. Ohgaki. Primary and secondary glioblastomas: from concept to clinical diagnosis. *Neuro Oncol*, 1(1):44–51, Jan 1999.

[45] Juergen A Knoblich. Mechanisms of asymmetric stem cell division. *Cell*, 132(4):583–597, Feb 2008.

[46] Dan R Laks, Michael Masterman-Smith, Koppany Visnyei, Brigitte Angenieux, Nicholas M Orozco, Ian Foran, William H Yong, Harry V Vinters, Linda M Liau, Jorge A Lazareff, Paul S Mischel, Timothy F Cloughesy, Steve Horvath, and Harley I Kornblum. Neurosphere formation is an independent predictor of clinical outcome in malignant glioma. *Stem Cells*, 27(4):980–987, Jan 2009.

[47] Jeongwu Lee, Svetlana Kotliarova, Yuri Kotliarov, Aiguo Li, Qin Su, Nicholas M Donin, Sandra Pastorino, Benjamin W Purow, Neil Christopher, Wei Zhang, John K Park, and Howard A Fine. Tumor stem cells derived from glioblastomas cultured in bfgf and egf more closely mirror the phenotype and genotype of primary tumors than do serum-cultured cell lines. *Cancer Cell*, 9(5):391–403, May 2006.

[48] Keith L Ligon, Emmanuelle Huillard, Shwetal Mehta, Santosh Kesari, Hongye Liu, John A Alberta, Robert M Bachoo, Michael Kane, David N Louis, Ronald A Depinho, David J Anderson, Charles D Stiles, and David H Rowitch. Olig2-regulated lineage-restricted pathway controls replication competence in neural stem cells and malignant glioma. *Neuron*, 53(4):503–517, Feb 2007.

[49] Sheila Alcantara Llaguno, Jian Chen, Chang-Hyuk Kwon, Erica L Jackson, Yanjiao Li, Dennis K Burns, Arturo Alvarez-Buylla, and Luis F Parada. Malignant astrocytomas originate from neural stem/progenitor cells in a somatic tumor suppressor mouse model. *Cancer Cell*, 15(1):45–56, Jan 2009.

[50] David N Louis, Hiroko Ohgaki, Otmar D Wiestler, Webster K Cavenee, Peter C Burger, Anne Jouvet, Bernd W Scheithauer, and Paul Kleihues. The 2007 who classification of tumours of the central nervous system. *Acta Neuropathol*, 114(2):97–109, Aug 2007.

[51] Subha Madhavan, Jean-Claude Zenklusen, Yuri Kotliarov, Himanso Sahni, Howard A Fine, and Kenneth Buetow. Rembrandt: helping personalized medicine become a reality through integrative translational research. *Mol Cancer Res*, 7(2):157–167, Feb 2009.

[52] E. Maiorano, G. Favia, S. Pece, L. Resta, P. Maisonneuve, P. P. Di Fiore, S. Capodiferro, U. Urbani, and G. Viale. Prognostic implications of numb immunoreactivity in salivary gland carcinomas. *Int J Immunopathol Pharmacol*, 20(4):779–789, 2007.

[53] Lucia Di Marcotullio, Elisabetta Ferretti, Azzura Greco, Enrico De Smaele, Agnese Po, Maria Anna Sico, Maurizio Alimandi, Giuseppe Giannini, Marella Maroder, Isabella Screpanti, and Alberto Gulino. Numb is a suppressor of hedgehog signalling and targets gli1 for itch-dependent ubiquitination. *Nat Cell Biol*, 8(12):1415–1423, Dec 2006.

[54] V. Marigo, D. J. Roberts, S. M. Lee, O. Tsukurov, T. Levi, J. M. Gastier, D. J. Epstein, D. J. Gilbert, N. G. Copeland, and C. E. Seidman. Cloning, expression, and chromosomal location of shh and ihh: two human homologues of the drosophila segment polarity gene hedgehog. *Genomics*, 28(1):44–51, Jul 1995.

[55] Melanie A McGill, Sascha E Dho, Gerry Weinmaster, and Catherine Jane McGlade. Numb regulates post-endocytic trafficking and degradation of notch1. *J Biol Chem*, Jun 2009.

[56] Melanie A McGill and C. Jane McGlade. Mammalian numb proteins promote notch1 receptor ubiquitination and degradation of the notch1 intracellular domain. *J Biol Chem*, 278(25):23196–23203, Jun 2003.

[57] E. G. Van Meir, T. Kikuchi, M. Tada, H. Li, A. C. Diserens, B. E. Wojcik, H. J. Huang, T. Friedmann, N. de Tribolet, and W. K. Cavenee. Analysis of the p53 gene and its expression in human glioblastoma cells. *Cancer Res*, 54(3):649–652, Feb 1994.

[58] Anastasia Murat, Eugenia Migliavacca, Thierry Gorlia, Wanyu L Lambiv, Tal Shay, Marie-France Hamou, Nicolas de Tribolet, Luca Regli, Wolfgang Wick, Mathilde C M Kouwenhoven, Johannes A Hainfellner, Frank L Heppner, Pierre-Yves Dietrich, Yitzhak Zimmer, J. Gregory Cairncross, Robert-Charles Janzer, Eytan Domany, Mauro Delorenzi, Roger Stupp, and Monika E Hegi. Stem cell-related "self-renewal" signature and high epidermal growth factor receptor expression associated with resistance to concomitant chemoradiotherapy in glioblastoma. *J Clin Oncol*, 26(18):3015–3024, Jun 2008.

[59] Jing Nie, Melanie A McGill, Matt Dermer, Sascha E Dho, Cheryl D Wolting, and C. Jane McGlade. Lnx functions as a ring type e3 ubiquitin ligase that targets the cell fate determinant numb for ubiquitin-dependent degradation. *EMBO J*, 21(1-2):93–102, Jan 2002.

[60] Takashi Nishimura, Yuko Fukata, Katsuhiro Kato, Tomoya Yamaguchi, Yoshiharu Matsuura, Hiroyuki Kamiguchi, and Kozo Kaibuchi. Crmp-2 regulates polarized numb-mediated endocytosis for axon growth. *Nat Cell Biol*, 5(9):819–826, Sep 2003.

[61] Toshiyuki Ohtsuka, Itaru Imayoshi, Hiromi Shimojo, Eiichiro Nishi, Ryoichiro Kageyama, and Susan K McConnell. Visualization of embryonic neural stem cells using hes promoters in transgenic mice. *Mol Cell Neurosci*, 31(1):109–122, Jan 2006.

[62] Salvatore Pece, Michela Serresi, Elisa Santolini, Maria Capra, Esther Hulleman, Viviana Galimberti, Stefano Zurrida, Patrick Maisonneuve, Giuseppe Viale, and Pier Paolo Di Fiore. Loss of negative regulation by numb over notch is relevant to human breast carcinogenesis. *J Cell Biol*, 167(2):215–221, Oct 2004.

[63] Petur H Petersen, Kaiyong Zou, Joseph K Hwang, Yuh Nung Jan, and Weimin Zhong. Progenitor cell maintenance requires numb and numblike during mouse neurogenesis. *Nature*, 419(6910):929–934, Oct 2002.

[64] Heidi S Phillips, Samir Kharbanda, Ruihuan Chen, William F Forrest, Robert H Soriano, Thomas D Wu, Anjan Misra, Janice M Nigro, Howard Colman, Liliana Soroceanu, P. Mickey Williams, Zora Modrusan, Burt G Feuerstein, and Ken Aldape. Molecular subclasses of high-grade glioma predict prognosis, delineate a pattern of disease progression, and resemble stages in neurogenesis. *Cancer Cell*, 9(3):157–173, Mar 2006.

[65] Steven M Pollard, Koichi Yoshikawa, Ian D Clarke, Davide Danovi, Stefan Stricker, Roslin Russell, Jane Bayani, Renee Head, Marco Lee, Mark Bernstein, Jeremy A Squire, Austin Smith, and Peter Dirks. Glioma stem cell lines expanded in adherent culture have tumor-specific phenotypes and are suitable for chemical and genetic screens. *Cell Stem Cell*, 4(6):568–580, Jun 2009.

[66] Benjamin W Purow, Raqeeb M Haque, Martha W Noel, Qin Su, Michael J Burdick, Jeongwu Lee, Tilak Sundaresan, Sandra Pastorino, John K Park, Irina Mikolaenko, Dragan Maric, Charles G Eberhart, and Howard A Fine. Expression of notch-1 and its ligands, delta-like-1 and jagged-1, is critical for glioma cell survival and proliferation. *Cancer Res*, 65(6):2353–2363, Mar 2005.

[67] Tracy-Ann Read, Marie P Fogarty, Shirley L Markant, Roger E McLendon, Zhengzheng Wei, David W Ellison, Phillip G Febbo, and Robert J Wechsler-Reya. Identification of cd15 as a marker for tumor-propagating cells in a mouse model of medulloblastoma. *Cancer Cell*, 15(2):135–147, Feb 2009.

[68] A. I. Saeed, V. Sharov, J. White, J. Li, W. Liang, N. Bhagabati, J. Braisted, M. Klapa, T. Currier, M. Thiagarajan, A. Sturn, M. Snuffin, A. Rezantsev, D. Popov, A. Ryltsov, E. Kostukovich, I. Borisovsky, Z. Liu, A. Vinsavich, V. Trush, and J. Quackenbush. Tm4: a free, open-source system for microarray data management and analysis. *Biotechniques*, 34(2):374–378, Feb 2003.

[69] Per Ø Sakariassen, Lars Prestegarden, Jian Wang, Kai-Ove Skaftnesmo, Rupavathana Mahesparan, Carla Molthoff, Peter Sminia, Eirik Sundlisaeter, Anjan Misra, Berit Bølge Tysnes, Martha Chekenya, Hans Peters, Gabriel Lende, Karl Henning Kalland, Anne M Øyan, Kjell Petersen, Inge Jonassen, Albert van der Kogel, Burt G Feuerstein, A. Jorge A Terzis, Rolf Bjerkvig, and Per Øyvind Enger. Angiogenesis-independent tumor growth mediated by stem-like cancer cells. *Proc Natl Acad Sci U S A*, 103(44):16466–16471, Oct 2006.

[70] A. E. Salcini, S. Confalonieri, M. Doria, E. Santolini, E. Tassi, O. Minenkova, G. Cesareni, P. G. Pelicci, and P. P. Di Fiore. Binding specificity and in vivo targets of the eh domain, a novel protein-protein interaction module. *Genes Dev*, 11(17):2239–2249, Sep 1997.

[71] E. Santolini, C. Puri, A. E. Salcini, M. C. Gagliani, P. G. Pelicci, C. Tacchetti, and P. P. Di Fiore. Numb is an endocytic protein. *J Cell Biol*, 151(6):1345–1352, Dec 2000.

[72] H. Sasaki, C. Hui, M. Nakafuku, and H. Kondoh. A binding site for gli proteins is essential for hnf-3beta floor plate enhancer activity in transgenics and can respond to shh in vitro. *Development*, 124(7):1313–1322, Apr 1997.

[73] Thomas D Schmittgen and Kenneth J Livak. Analyzing real-time pcr data by the comparative c(t) method. *Nat Protoc*, 3(6):1101–1108, 2008.

[74] Carlos A Scrideli, Carlos G Carlotti, Oswaldo K Okamoto, Vanessa S Andrade, Maria A A Cortez, Fábio J N Motta, Agda K Lucio-Eterovic, Luciano Neder, Sérgio Rosemberg, Sueli M Oba-Shinjo, Suely K N Marie, and Luíz G Tone. Gene expression profile analysis of primary glioblastomas and non-neoplastic brain tissue: identification of potential target genes by oligonucleotide microarray and real-time quantitative pcr. *J Neurooncol*, 88(3):281–291, Jul 2008.

[75] Miguel Sena-Esteves, Jessica C Tebbets, Sabine Steffens, Timothy Crombleholme, and Alan W Flake. Optimized large-scale production of high titer lentivirus vector pseudotypes. *J Virol Methods*, 122(2):131–139, Dec 2004.

[76] Alan H Shih and Eric C Holland. Notch signaling enhances nestin expression in gliomas. *Neoplasia*, 8(12):1072–1082, Dec 2006.

[77] Vasily Shinin, Barbara Gayraud-Morel, Danielle Gomès, and Shahragim Tajbakhsh. Asymmetric division and cosegregation of template dna strands in adult muscle satellite cells. *Nat Cell Biol*, 8(7):677–687, Jul 2006.

[78] Sheila K Singh, Ian D Clarke, Mizuhiko Terasaki, Victoria E Bonn, Cynthia Hawkins, Jeremy Squire, and Peter B Dirks. Identification of a cancer stem cell in human brain tumors. *Cancer Res*, 63(18):5821–5828, Sep 2003.

[79] Sheila K Singh, Cynthia Hawkins, Ian D Clarke, Jeremy A Squire, Jane Bayani, Takuichiro Hide, R. Mark Henkelman, Michael D Cusimano, and Peter B Dirks. Identification of human brain tumour initiating cells. *Nature*, 432(7015):396–401, Nov 2004.

[80] Christian A Smith, Kimberly M Lau, Zohra Rahmani, Sascha E Dho, Greg Brothers, Ye Min She, Donna M Berry, Eric Bonneil, Pierre Thibault, François Schweisguth, Roland Le Borgne, and C. Jane McGlade. apkc-mediated phosphorylation regulates asymmetric membrane localization of the cell fate determinant numb. *EMBO J*, 26(2):468–480, Jan 2007.

[81] R. Staden. The staden sequence analysis package. *Mol Biotechnol*, 5(3):233–241, Jun 1996.

[82] Roger Stupp, Monika E Hegi, Warren P Mason, Martin J van den Bent, Martin J B Taphoorn, Robert C Janzer, Samuel K Ludwin, Anouk Allgeier, Barbara Fisher, Karl Belanger, Peter Hau, Alba A Brandes, Johanna Gijtenbeek, Christine Marosi, Charles J

Vecht, Karima Mokhtari, Pieter Wesseling, Salvador Villa, Elizabeth Eisenhauer, Thierry Gorlia, Michael Weller, Denis Lacombe, J. Gregory Cairncross, René-Olivier Mirimanoff, European Organisation for Research, Treatment of Cancer Brain Tumour, Radiation Oncology Groups, and National Cancer Institute of Canada Clinical Trials Group. Effects of radiotherapy with concomitant and adjuvant temozolomide versus radiotherapy alone on survival in glioblastoma in a randomised phase iii study: 5-year analysis of the eortc-ncic trial. *Lancet Oncol*, 10(5):459–466, May 2009.

[83] Roger Stupp, Warren P Mason, Martin J van den Bent, Michael Weller, Barbara Fisher, Martin J B Taphoorn, Karl Belanger, Alba A Brandes, Christine Marosi, Ulrich Bogdahn, Jürgen Curschmann, Robert C Janzer, Samuel K Ludwin, Thierry Gorlia, Anouk Allgeier, Denis Lacombe, J. Gregory Cairncross, Elizabeth Eisenhauer, René O Mirimanoff, European Organisation for Research, Treatment of Cancer Brain Tumor, Radiotherapy Groups, and National Cancer Institute of Canada Clinical Trials Group. Radiotherapy plus concomitant and adjuvant temozolomide for glioblastoma. *N Engl J Med*, 352(10):987–996, Mar 2005.

[84] Kazutoshi Takahashi, Koji Tanabe, Mari Ohnuki, Megumi Narita, Tomoko Ichisaka, Kiichiro Tomoda, and Shinya Yamanaka. Induction of pluripotent stem cells from adult human fibroblasts by defined factors. *Cell*, 131(5):861–872, Nov 2007.

[85] Frits Thorsen, Daniel Jirak, Jian Wang, Eva Sykova, Rolf Bjerkvig, Per Øyvind Enger, Albert van der Kogel, and Milan Hajek. Two distinct tumor phenotypes isolated from glioblastomas show different mrs characteristics. *NMR Biomed*, 21(8):830–838, Oct 2008.

[86] Jo Vandesompele, Katleen De Preter, Filip Pattyn, Bruce Poppe, Nadine Van Roy, Anne De Paepe, and Frank Speleman. Accurate normalization of real-time quantitative rt-pcr data by geometric averaging of multiple internal control genes. *Genome Biol*, 3(7):RESEARCH0034, Jun 2002.

[87] J. M. Verdi, A. Bashirullah, D. E. Goldhawk, C. J. Kubu, M. Jamali, S. O. Meakin, and H. D. Lipshitz. Distinct human numb isoforms regulate differentiation vs. proliferation in the neuronal lineage. *Proc Natl Acad Sci U S A*, 96(18):10472–10476, Aug 1999.

[88] Jian Wang, Per Ø Sakariassen, Oleg Tsinkalovsky, Heike Immervoll, Stig Ove Bøe, Agnete Svendsen, Lars Prestegarden, Gro Røsland, Frits Thorsen, Linda Stuhr, Anders Molven, Rolf Bjerkvig, and Per Ø Enger. Cd133 negative glioma cells form tumors in nude rats and give rise to cd133 positive cells. *Int J Cancer*, 122(4):761–768, Feb 2008.

[89] Britta Westhoff, Ivan N Colaluca, Giovanni D'Ario, Maddalena Donzelli, Daniela Tosoni, Sara Volorio, Giuseppe Pelosi, Lorenzo Spaggiari, Giovanni Mazzarol, Giuseppe Viale, Salvatore Pece, and Pier Paolo Di Fiore. Alterations of the notch pathway in lung cancer. *Proc Natl Acad Sci U S A*, 106(52):22293–22298, Dec 2009.

[90] Qijin Xu, Xiangpeng Yuan, Gentao Liu, Keith L Black, and John S Yu. Hedgehog signaling regulates brain tumor-initiating cell proliferation and portends shorter survival

for patients with pten-coexpressing glioblastomas. *Stem Cells*, 26(12):3018–3026, Dec 2008.

[91] Benedict Yan, Feroz Mohd Omar, Kakoli Das, Wai Hoe Ng, Chinghway Lim, Koh Shiuan, Celestial T Yap, and Manuel Salto-Tellez. Characterization of numb expression in astrocytomas. *Neuropathology*, 28(5):479–484, Oct 2008.

[92] Satomi Yogosawa, Yasuhiro Miyauchi, Reiko Honda, Hirofumi Tanaka, and Hideyo Yasuda. Mammalian numb is a target protein of mdm2, ubiquitin ligase. *Biochem Biophys Res Commun*, 302(4):869–872, Mar 2003.

[93] Chen Zhao, Alan Chen, Catriona H Jamieson, Mark Fereshteh, Annelie Abrahamsson, Jordan Blum, Hyog Young Kwon, Jynho Kim, John P Chute, David Rizzieri, Michael Munchhof, Todd Vanarsdale, Philip A Beachy, and Tannishtha Reya. Hedgehog signalling is essential for maintenance of cancer stem cells in myeloid leukaemia. *Nature*, Jan 2009.

[94] Hongwu Zheng, Haoqiang Ying, Haiyan Yan, Alec C Kimmelman, David J Hiller, An-Jou Chen, Samuel R Perry, Giovanni Tonon, Gerald C Chu, Zhihu Ding, Jayne M Stommel, Katherine L Dunn, Ruprecht Wiedemeyer, Mingjian J You, Cameron Brennan, Y. Alan Wang, Keith L Ligon, Wing H Wong, Lynda Chin, and Ronald A DePinho. p53 and pten control neural and glioma stem/progenitor cell renewal and differentiation. *Nature*, 455(7216):1129–1133, Oct 2008.

[95] S. Zhou, J. D. Schuetz, K. D. Bunting, A. M. Colapietro, J. Sampath, J. J. Morris, I. Lagutina, G. C. Grosveld, M. Osawa, H. Nakauchi, and B. P. Sorrentino. The abc transporter bcrp1/abcg2 is expressed in a wide variety of stem cells and is a molecular determinant of the side-population phenotype. *Nat Med*, 7(9):1028–1034, Sep 2001.

A. Appendix

A.1. Manufacturers and suppliers

Abcam Abcam, Cambridge, MA, USA
Addgene Addgene, Cambridge, MA, USA
Amersham Amersham plc, Amersham, UK
Applied Biosystems Applied Biosystems, Foster City, CA, USA
BD Biosciences BD Biosciences, Franklin Lakes, NJ, USA
Beckman Coulter Beckman Coulter, Fullerton, CA, USA
BioChain BioChain, Hayward, CA, USA
Bio-Rad Bio-Rad, Hercules, CA, USA
Bruker Bruker Biospin, Ettlingen, Germany
Dako Dako, Glostrup, Denmark
Fermentas Fermentas, Burlington, Canada
Finnzymes Finnzymes, Espoo, Finland
FujiFilm FujiFilm, Tokyo, Japan
GeneTex GeneTex, Irvine, CA, USA
Hamilton Hamilton, Reno, NV, USA
Invitrogen Invitrogen, Carlsbad, CA, USA
Invivogen Invivogen, San Diego, CA, USA
Leica Leica, Wetzlar, Germany
Lonza Lonza, Basel, Switzerland
Millipore Millipore, Billerica, MA, USA
MJ Research MJ Research, Waltham, MA, USA
MP Biomedicals MP Biomedicals, Solon, OH, USA
Nikon Nikon, Tokyo, Japan
Orion Pharma Orion Pharma, Espoo, Finland
PAA PAA, Pasching, Austria
Pall Corporation Pall Corporation, Ann Arbor, MI, USA
Peprotech Peprotech, Rocky Hill, NJ, USA

Pfizer Pfizer, New York, NY, USA
Promega Promega, Madison, WI, USA
Qiagen Qiagen, Hilden, Germany
Ratiopharm Ratiopharm, Ulm, Germany
Roche Roche, Basel, Switzerland
Sakura Sakura, Zoeterwoude, Netherlands
Santa Cruz Santa Cruz Biotechnology, Santa Cruz, CA, USA
Schering-Plough Schering-Plough, Kenilworth, NJ, USA
Sigma Sigma Aldrich, St. Louis, MO, USA
SPSS SPSS, Chicago, IL, USA
StemCell Technologies StemCell Technologies, Vancouver, Canada
Thermo Scientific Thermo Fisher Scientific, Waltham, MA, USA
Vector Labs Vector Laboratories, Burlingame, CA, USA
Zeiss Zeiss, Jena, Germany
Zymed Zymed, San Francisco, CA, USA

A.2. Plasmid map

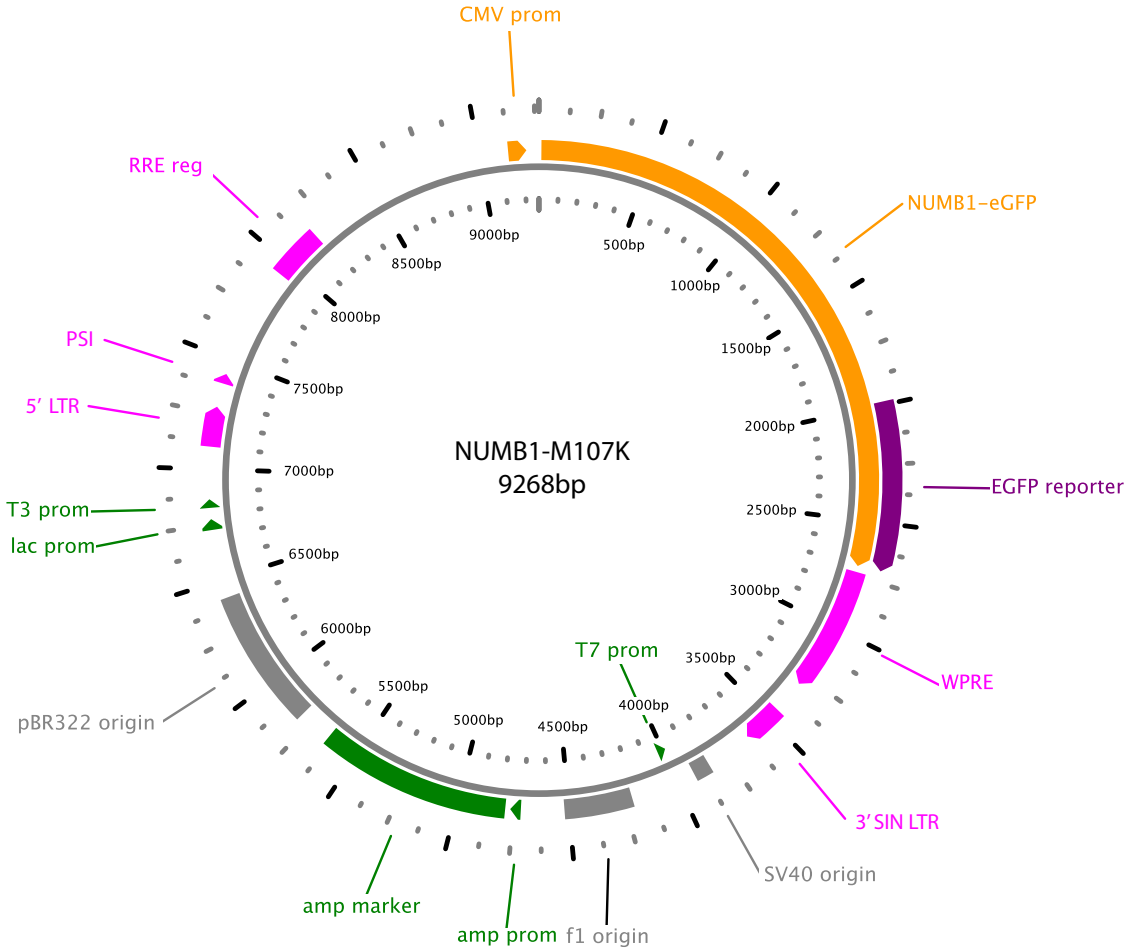

Figure A.1.: **Plasmid map of NUMB1-M107K** Vectors for NUMB2, NUMB3 and NUMB4 are analogous and identical except for the respective NUMB coding sequence. All vectors are derived from M107 (pRRL.sinCMVeGFPpre).

A.3. Virus batches

Titers of viral supernatants are listed in Table A.1.

batch	medium	concentrated	NUMB1-GFP	NUMB2-GFP	NUMB3-GFP	NUMB4-GFP	GFP
16.05.2008	PBS	yes	-	2.72×10^{7}	-	1.38×10^{7}	3.08×10^{7}
24.07.2008	OptiMEM	yes	-	1.12×10^{8}	-	1.30×10^{8}	3.36×10^{8}
25.08.2008	DMEM	no	-	1.91×10^{5}	-	1.40×10^{5}	2.13×10^{6}
22.05.2009	OptiMEM	no	7.43×10^{5}	7.50×10^{5}	7.59×10^{5}	1.12×10^{6}	1.38×10^{6}

Table A.1.: **Titers of viral supernatants** Viral supernatants were harvested in the indicated medium or, if concentrated by ultracentrifugation, resuspended in the indicated medium. Titration was done in duplicates on U87 cells and transduction efficiency was determined by flow cytometric analysis of GFP expression.

Curriculum vitae

Mein Lebenslauf wird aus Gründen des Datenschutzes in der elektronischen Fassung meiner Arbeit nicht veröffentlicht.